QUILL
Quarterly Reports

November 2022 – January 2023

CONFIDENTIAL (up to February 2026)

Contents

QUILL Quarterly Report

November 2022 – January 2023

Name:	Haris Amir		
Supervisor(s):	Professor John Holbrey		
Position:	Postgraduate PhD		
Start date:	10/01/2020	**Anticipated end date:**	30/09/2024
Funding body:	ESPRC/UKRI		

Design of New, Non-coordinating, and Hydrophobic Anions for Functional Ionic Liquids

Boron containing anions are of interest for the development of new ionic liquid anions with a wide range of potential applications including electro- and photo- chemistry, and for separation and extraction of metals and waste. In this work, functional borate anions formed as complexes with O/N-chelators for ionic liquid applications have been designed and investigated.

After synthesis, characterisation, and investigation of the library of O/N-chelated borate anions formulated as ionic liquids described previously, borate anions containing N-coordinated groups have been investigated, building on the known tetrakis(1-imidazoly)borate, to explore whether this and related functional anions are suitable for translation into ionic liquids. It has been suggested, based on density functional calculations that azolium poly(azolyl)borate ionic liquids might be effective media for reversible capture of SO_2, although the target ionic liquids are not known *ex silico*.[1] From the borate anions described in the theoretical screening study, four were chosen for synthesis and evaluation for potential to form ionic liquids and for to gas solubility. The heterocycles targeted for use to form 4-coordinate borate anions are shown in figure 1.

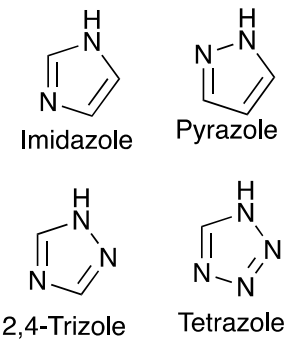

Figure 1 - The structures of the heterocycles chosen to synthesise borate anions

The crystals (figure 2) that formed during the synthesis of Sodium tetrakis(1-imidazoly)borate, $Na[B(Im)_4]$, was found to be unreacted imidazole as the crystals melted around 85˚C.

Figure 2 - An aerial view of the crystals formed.

The reaction shown in scheme 1 was repeated,[2] this time with pyrazole to form $Na[B(Pz)_4]$, similar crystals were formed during the reaction. The crystals were again found to be unreacted starting material, in this case pyrazole as the melting point was observed to be 68˚C.

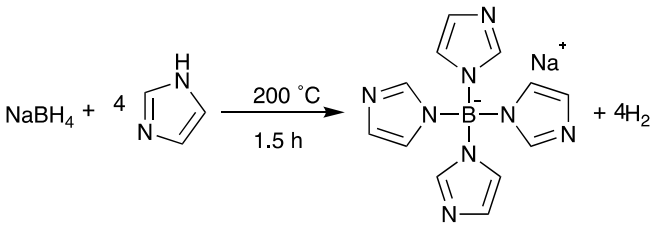

Scheme 1 - Reaction scheme for the synthesis of $Na[B(Im)_4]$

Thermogravimetric analysis (TGA) of the crude $Na[B(Pz)_4]$ was recorded to determine the thermal properties of the salt, the TGA graph can be seen in figure 3.

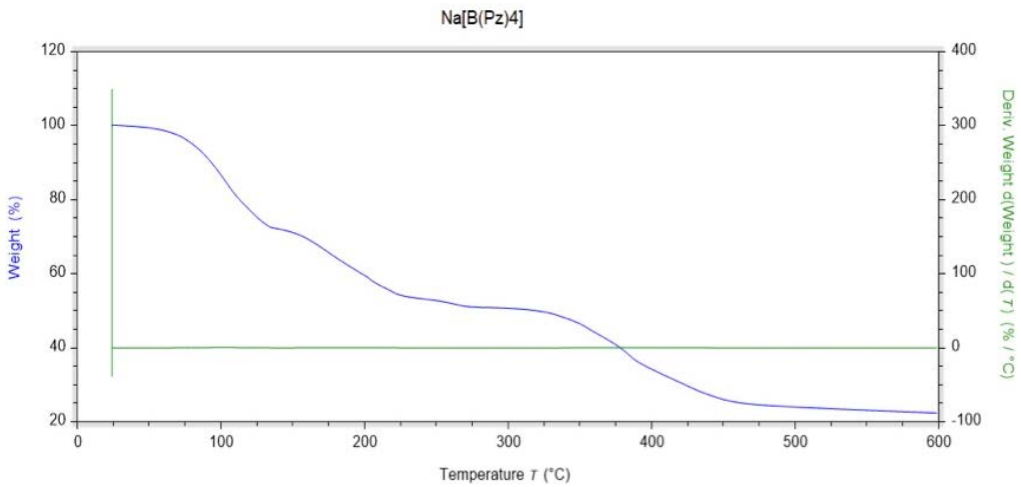

Figure 3 - TGA of crude $Na[B(Pz)_4]$ 5˚C/min

The TGA shows weight loss close to 100˚C this is likely to be the residual ethanol on the crude product there is also significant weight loss between 100 – 200˚C, this weight loss is likely a result of any remaining pyrazole from the reaction. As a result of this it is difficult to determine the thermal properties of $Na[B(Pz)_4]$, from previous the onset temperature (temperature of when product decomposes) is expected to be between 200 – 300˚C as B-N bonds have been found to be stronger. Purification of $Na[B(Pz)_4]$ and $Na[B(Im)_4]$ will be carried out to obtain a more accurate representation of the thermal properties these borate salts hold.

Purification *via* recrystallisation of $Na[B(Pz)_4]$ and $Na[B(Im)_4]$ was carried, crystals of $Na[B(Pz)_4]$ were successfully grown and were at a sufficient quality to perform single crystal XRD, figure 4 shows the crystal structure obtained from the single XRD.

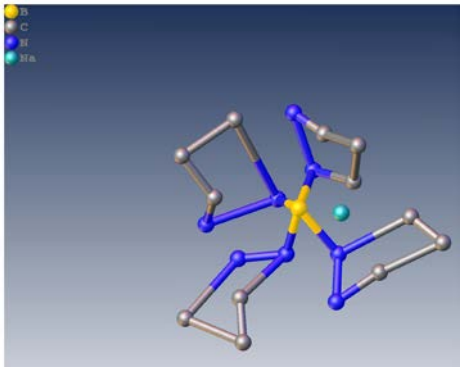

Figure 4 - Crystal structure of $Na[B(Pz)_4]$

It was expected that the two of the pyrazole rings will lay flat along the plane, one will be in-front, and one will be behind the plane. Figure 4 doesn't show what was expected, instead it shows the pyrazole rings are twisted and bent, this suggests that there is either disorder or twinning in the crystal structure. Disorder in a crystal structure is when there is crystallisation of more than one rotamer, conformer or isomer, a consequence of disorder is the crystallographic solution is the sum of the various forms. Twinning occurs when two or more adjacent crystals are oriented so that they share some of the same lattice points in a symmetrical manner. These factors affect the diffraction when measuring single crystal XRD and thus giving an inaccurate crystal structure of the product.

Future work will include the full characterisation of $Na[B(Pz)_4]$ and $Na[B(Im)_4]$ which includes NMR, TGA, single crystal XRD and differential scanning calorimetry (DSC). The reaction in scheme 1 will also be repeated using 1,2,4-trizole and tetrazole, once the 4 sodium salts have been synthesised and characterised the next step will be to synthesise ionic liquids *via* ionic exchange with $[C_4mim]Cl$ and $[P_{66614}]Cl$.

References

1. H. Tang, and D. Lu, ChemPhysChem., 2015., **16**., 2854-2860.
2. H. B. Hamilton, A. K. Kelly, W. Malasi, and J. C. Ziegler, Inorg. Chem., 2003, **42**, 9, 3067–3073.

QUILL Quarterly Report

November 2022 – January 2023

Name:	Dominic Burns		
Supervisor(s):	Prof John Holbrey, Prof Gosia Swadzba-Kwasny and Dr Hye-Kyung Timken		
Position:	PhD Student		
Start date:	1st October 2019	**Anticipated end date:**	31st May 2023
Funding body:	EPSRC		

Recycle and Reuse of Process Water Through Sulfate Removal: Developing an Ionic Liquid Technology for Selective Anion Recognition and Extraction

Background

This is an EPSRC industrial CASE project in collaboration with Chevron, to explore liquid technologies for the treatment of saline process water with the initial objective of selective sulfate removal from highly competitive aqueous streams. Initial work began by characterising a series of long chain tetraalkyl ammonium and phosphonium chlorides with functionalities that mimic solid ion-exchange resins and that are shown to extract sulfate via an ion-exchange (IX) mechanism. The main driving force for this process is the electrostatic attraction of sulfate towards the cationic centre however, when chloride is already present in the aqueous phase this blocks the exchange process reducing the extraction significantly. Building on this, it has also been shown before that the addition of weak anion receptors can enhance the removal of sulfate by chelation.

Lastly, I have also been working with Chevron on a CO2 capture project using ionic liquids since July 2022 however, the details of this work cannot be disclosed at this time.

Objective of this work

Main objective of this work is to develop a strategy for the selective removal of aqueous sulfate from competitive waste-water streams. A secondary objective is now the use of ionic liquids for CO_2 capture.

Progress to date

As I am in the last few month of my PhD it is time to wrap up. Most of my effort is now being split between finishing the last of the ionic liquid chlorides for liquid-liquid anion exchange, this ionic liquid has a ethyl hydroxy functionality that mimics the functionality found in strongly basic type II resins. A schematic of the synthetic route is shown in figure 1. Due to the use of ethylene oxide this reaction took a lot of planning and contact with health and safety. The reaction was carried out in 4 batches of approx. 50 mL scale. The product can be purified by crystallisation from ethyl acetate or a mixture of acetone-diethyl ether as is currently being attempted. If this fails a flash column chromatography can be done first using ethyl acetate to elute the starting material, then switching to acetonitrile with 5% acetic acid to elute the product is shown by the TLC's in figure 2.

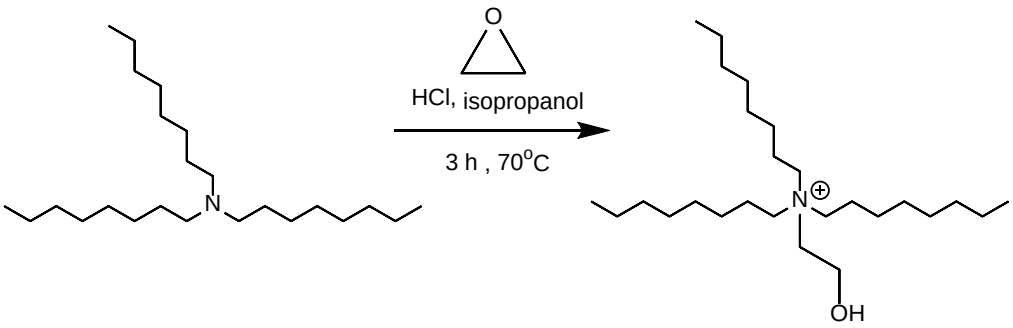

Figure 1 - Synthetic route to the ionic liquid [N_{2OH888}]Cl.

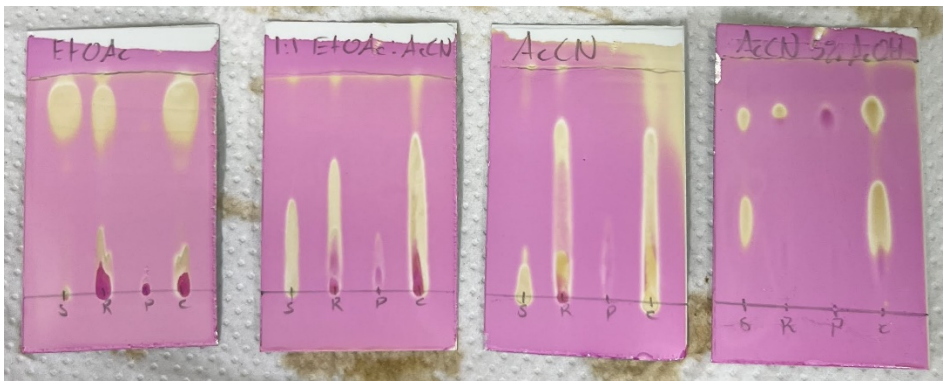

Figure 2 - Silica gel TLC plates showing how using a gradient solvent system of ethyl acetate to acetonitrile 5% acetic acid can be used to purify [N_{2OH888}]Cl.

All the above is required to finish Chapter 1 of my thesis and a first paper. Chapter 2 will lead directly on from this and involves the addition of simple anion receptors into the ionic liquids to enhance the IX process. The structures of these receptors is shown in figure 3.

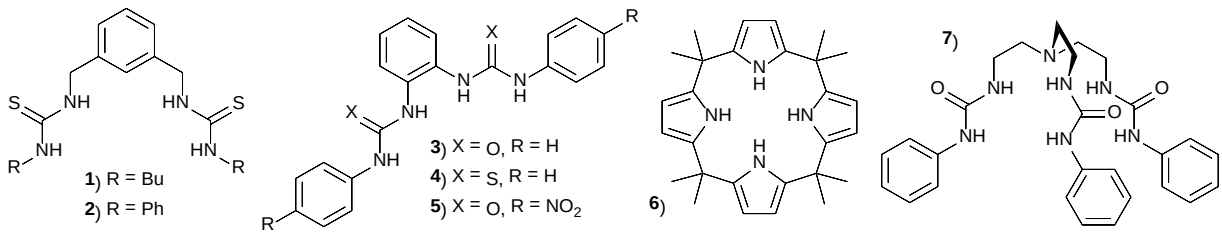

Figure 3 - Structures of the anion receptors used to enhance the ion-exchange process for sulfate removal described above.

To date all the receptors have been synthesised and current work involves adding them to Aliquat 336 to improve the IX process. Two binding studies also need to be done for each receptor to quantify the binding affinity for sulfate and chloride. Preliminary studies have shown that in DMSO, the receptors bind stronger to chloride yet they still improve the sulfate removal and so it is hypothesised that the opposite is true in the ionic liquid phase, that is, that the receptor binds sulfate stronger than chloride so a binding study in an ionic liquid phase has been devised but is currently on hold until Chapter 1 and 3 are finished.

Conclusions and future work

Future work: finish my PhD. Need to complete this last ionic liquid chloride that will complete my data set for a paper on sulfate removal and the first chapter of my thesis. Finishing chapter 2 and hopefully a second paper will involve a lot of anion binding studies and desperate crystallisation attempts. Chapter 3 will be on the CO2 capture project.

QUILL Quarterly Report

November 2022 – January 2023

Name:	Oguzhan CAKIR		
Supervisor(s):	Professor Peter Nockemann		
Position:	PhD student		
Start date:	05/01/2023	**Anticipated end date:**	31/12/2025
Funding body:	Turkish Government (TENMAK)		

Magneto-Structural Properties of Boron-containing Rare-Earth Magnets Synthesised Through Ionic Liquid Pathways

Background

Molecular nanoclusters constitute an intermediate state of matter between molecules and nanoparticles. The advantage of these materials is that, in contrast to conventional nanoparticles, they have a defined molecular structure that can exhibit cooperative spin-spin interactions, which might be used for magnetic high-density data-storage on a molecular level. We propose to investigate the synthesis of novel and interesting molecular cluster magnets using ionic liquid pathways; the aim is to achieve control over magnetic materials at cluster size with defined structures by using ground-breaking new synthetic methodologies.

Molecular cluster magnets provide a rich playground of different magnetic interactions in well-defined nanostructures, occupying the space between the quantum and classical world. Other interesting possibilities are clusters with antiferromagnetic or ferromagnetic intra-molecular couplings, which may exhibit bulk ferro- or ferrimagnetic interactions. Studying their physical properties contributes to our understanding of magnetic interactions in complex molecular structures. The use of ionic liquids allows for fundamentally different synthetic pathways resulting in compounds not accessible through conventional solvent-based synthesis.

Objective of this work

- Synthesise novel molecular cluster magnets with spin-cooperative behaviour using ionic liquid pathways
- Understand synthesis of molecular cluster magnets through ionic liquid pathways including the formation mechanism
- The magneto structural properties of both the liquid precursor and the solid-state molecular cluster magnets as a function of varying syntheses conditions.
- Use the understanding of formation mechanisms and magneto structural property relationships to inform the design of further molecular cluster magnets

Progress to date

A training plan and training content required for my scholarship position were created and submitted to the institution.

Conclusions and future work

We started researching on the subject for a literature review. At the beginning of April, I will prepare and present a presentation about my doctoral work. The core ambition of this proposal is to understand and control ionic liquid synthesis of molecular cluster magnets. The long-term goal is to establish low-temperature solid-state chemistry of nanoclusters in ionic liquids as part of the toolbox of inorganic and materials chemists, disseminating gained knowledge in well-recognized high-impact publications. It is expected, that this will become the foundation for the development of new technologies.

QUILL Quarterly Report

November 2022 – January 2023

Name:	Edwin Harvey		
Supervisor(s):	Dr Oana Istrate, Prof Peter Nockemann and Dr Stephen Glover		
Position:	PhD Student		
Start date:	February 2022	**Anticipated end date:**	August 2025
Funding body:	Department for the Economy		

3D-Printable Redox Flow Battery Electrodes

Background

Redox flow batteries (RFBs) are promising candidates for grid-scale energy storage and stationary energy storage applications. They have a longer cycle life than lithium-ion and can use cheaper, safer, and more environmentally friendly electrolytes. Such systems are becoming more important as we rely more on intermittent renewable energy, such as wind and solar, as we move towards reaching net zero by 2050 (UK govt target).

The RFB design has not changed much since their inception in the 20th century (e.g. vanadium RFBs were invented in 1986 at the University of New South Wales, Australia). Electrodes are still typically made using carbon felt as these have good electrical conductivity, electrochemical activity, and are mechanically and chemically stable. However, using carbon felt as an electrode material limits cell design and is associated with a high interphase electrical resistance. Additionally, for flow-over electrode designs, flow channels must be machined into graphite plates which is complex and expensive. 3D-printable electrodes may offer a greater design freedom where, for example, flow channels can be printed as part of the design, and porous and solid elements can be combined.

Graphene nanocomposite materials may be able to replace graphite and carbon felt as an electrode material. Possible 3D-printing technologies for this material are fused deposition modelling (FDM), and stereolithography (SLA). FDM uses a heated thermoplastic filament which is extruded out of the printer nozzle, following a pre-calculated path to manufacture the part layer by layer. Graphene based nanocomposites have been printed using FDM but often suffer from agglomeration of graphene due to extruding conditions. SLA uses a liquid resin which is cured using UV light at the desired locations, also building the part layer by layer. SLA may offer improved graphene dispersion compared to FDM.

Objective of this work

To create a viable redox flow battery (RFB) electrode that has been manufactured through 3D-printing technology.

Progress to date

Initially, I spent time reading literature and planning my PhD by splitting it into work-packages that each last a few months. My first work-package is focused on manufacturing a 3D-printable RFB material utilising carbon nanofillers. After analysing the properties of various

polymer matrices, I have decided to focus on acrylate-based monomers that can be polymerised in-situ with graphene. This is because various papers have shown this method to produce high electrical conductivity and excellent graphene dispersion.

During initial experimental work graphene oxide (GO) was synthesised using a modified Hummers' method. Following this, seven polymer/graphene nanocomposites were manufactured using SLA 3D-printing containing GO and graphene nanoplatelet (GNP) fillers. Nanofillers and nanocomposites were then characterised using FTIR, Raman spectroscopy, X-ray diffraction, tensile testing, and electrical testing. A literature study and experimental work were submitted as part of my differentiation which was completed in November 2022.

Since November, I have been focused on manufacturing and modifying graphite powder and developing my characterisation skills. I have been undertaking an in-situ polymerisation method to produce high electrical conductivity nanocomposites which have the potential to be used as a 3D-printed electrode material.

Conclusions and future work

More graphene in-situ polymerisation experiments are planned, aiming to improve electrical properties further and simplify the procedure. I will then look at reprocessing the nanocomposites into filament that can be printed using fused deposition modelling (FDM). A review paper on flow-over vs flow-through cell architectures is also planned for the next few months.

QUILL Quarterly Report

November 2022 – January 2023

Name:	Aloisia King		
Supervisor(s):	Prof John Holbrey and Prof Małgorzata Swadźba-Kwaśny		
Position:	PhD student		
Start date:	01 October 2021	**Anticipated end date:**	March 2024
Funding body:	EPSRC		

Intrinsic FLP Systems in Ionic Liquids

Background

Frustrated Lewis acid/base pairs (FLPs) are potential metal-free alternatives to platinum group metal catalysts and have been shown to activate hydrogen for hydrogenation chemistry [1]. Typical examples of FLPs that have been studied are combinations of a sterically hindered bulky phosphine Lewis base paired with a strongly electrophilic Lewis acidic susbstituted borane. While many of the advances in FLP chemistry have sought to exploit these bulky phosphine/borane pairs, less attention has been given to alternative acid/base pairs although examples with non-boron Lewis acid FLP components are known, including N-methylacridinium salts that have been show to exhibit FLPs chemistry when paired with lutidine (2,6-dimethylpyridine) in solution [2].

Objective of this work

The goal of this research is to develop organic FLPs (eliminating the need for group 13-based Lewis acids) that are intrinsically also ionic liquids, using skills in ionic liquid design and engineering to generate new, novel IL-FLPs with potentially high active catalyst concentrations. This will allow chemistry using FLP catalysts to be intensified creating greener, sustainable chemistry through facile synthesis and replacement of both conventional solvents and platinum group metal catalysts.

Progress to date

Synthesis: Challenging synthesis of new *N*-alkyl-acridinium salts from sterically hindered acridine have been undertaken. In addition to successful synthesis of known N-methyl and N-benzylacridinium cations and their transformation into new ionic liquid salts with *bis*{trifluoromethylsulfonyl}imide ($[NTf_2]^-$) anions, methods have been developed to successfully synthesise new *N*-propylacridinium iodide, *N*-propylacridinium [NTf_2], *N*-butylacridinium butylsulfate, *N*-butylacridinium [NTf_2], *N*-benzylacridinium bromide and *N*-benzylacridinium [NTf_2] salts.

Solubility: The *N*-alkylacridinium *bis*{trifluoromethylsulfonyl}imide ([R-Ac][NTf_2]) salts synthesised are highly soluble in protonated H-lutidinium and H-picolinium *bis*{trifluoromethylsulfonyl}imide ([H-lut][NTf_2] and [H-pic][NTf_2]) ionic liquids. This contrasts with the poor and limiting solubility of *N*-methylacridinium salts in organic solvents [2] and suggests that ionic liquids in general could be good solvents to study reactions of these FLPs, as well as demonstrating the ability to form liquid FLP mixtures from stoichiometric

combinations of [R-Ac][NTf_2] salts as a Lewis acid and H-lutidine as a Lewis base. Phase behaviour of mixtures of [Me-Ac][NTf_2] + H-lutidine and H-lutidinum [NTf_2] + hydro-methylacridine across their composition ranges, representing the initial and final compositions of complete H_2 splitting and combination with the IL-FLP components have been characterised, demonstrating potential to generate an ionic liquid compositions from starting point to products.

Hydrogen Capture: Hydrogen-gas uptake screening experiments, initiated previously are still under detailed investigation. [Me-Ac][Tf_2N]/lutidine mixtures readily absorbed low pressure gaseous H_2 generating mixtures that show proton NMR signals assignable to formation of the hydro-methylacridine molecular adduct (addition of a hydride) and collapse of the lutidine signals into bulk IL H-lutidinium cations (protonation). Since the last report, experiments have been made to quantify gas uptake through monitoring the head-space H_2 concentration above the FLP using GC and ^{1}H NMR spectroscopy pre- and post-activation.

Conclusions and future work

In proof of concept, the ability to mix [Me-Ac][Tf_2N] and lutidine as a frustrated Lewis pair in the form of an ionic liquid/heterocycle pair in which the corresponding hydro-methylacridine/[H-lut][[NTf_2] H_2-adduct composition is also an ionic liquid/heterocycle pair have been demonstrated. Hydrogen uptake by [Me-Ac][Tf_2N]/lutidine pairs has been observed, with formation of the adduct species in a mixture. The range of know N-alkylacridinium salts know has been extended, adding C2, C3, and C4-alkyl substituents to the sterically hindered and difficult to alkylate acridine ring. It is anticipated that these new N-alkylacridinium cations will enable greater control of the available liquid range and freezing points of [R-Ac][NTf_2]/lutidine FLPs under investigation following established effects of N-alkyl substitution on melting points of organic IL salts [3] and generate LA components that are more sterically hindered increasing activation of small molecules. A draft communication of this initial work is in progress for submission, pending finalisation of H_2 activation results. We also plan to test the [Me-Ac][Tf_2N]/ lutidine system with a substrate and see if it is capable of acting as a catalyst.

References

1. D. W. Stephan and G. Erker, *Angew. Chem. Int. Ed.,* 2010, 49, 46–76.
2. E. R. Clark and M. J. Ingleson, *Angew. Chem., Int. Ed*., 2014, 53, 11306–11309.
3. C. Hardacre, J. D. Holbrey, C. L. Mullan, M. Nieuwenhuyzen, W. M. Reichert, K. R. Seddon and S. J. Teat, *New J. Chem.,* 2008, 1953-1967.

QUILL Quarterly Report

November 2022 – January 2023

Name:	Sanskrita Madhukailya		
Supervisor(s):	Professor John Holbrey and Dr. Leila Moura		
Position:	2nd year PhD student		
Start date:	19th April 2021	**Anticipated end date:**	20th April 2024
Funding body:	Tezpur University/QUB joint PhD scholarship		

LCST Behaviour in 5-Phenyltetrazolate Based Ionic Liquids

Background

In the previous report, the synthesis of ammonium ionic liquids of the type $[N_{444n}][PhTet]$, where n= 4,5,6,8 and $[N_{6666}][PhTet]$ along with a diphosphonium ionic liquid, 1,8-octanediyl-bis(tri-n-butylammonium)di(5-phenyltetrazolate) were carried out. In addition to that, the phase behaviour for a 50wt% composition of the prepared dicationic liquid was carried out using Crystal 16.

Objective of this work

The ultimate aim of this work is to understand and explain the lower critical solubility temperature (LCST) phase behaviour of some ionic liquids, to know the boundaries and frame a methodology for synthesising such ionic liquids that can behave as a potential draw solute to be used in the forward osmosis process for sea water desalination. In this process, a range of ionic liquids with the tetrazole moiety will be synthesised, tested, and compared with the existing ones, based on the type of anion or cation chosen, that can affect the phase behaviours.

Progress to date

1. The synthesised ammonium ionic liquids were tested for their phase behaviour, and it was found that the ionic liquids $[N_{4445}][PhTet]$, $[N_{4448}][Phtet]$ shows LCST at temperatures 5°C and 1°C respectively.

2. Further, detailed phase studies were done on 1,8-octanediyl-bis(tri-n-butylammonium)di(5-phenyltetrazolate) for compositions 2wt% up to 60wt% and was found to show LCST properties for the same.

3. Synthesis of few other dicationic ionic liquids, 1,4-butanediyl-bis(tri-n-butylammonium)di(5-phenyltetrazolate) (**1**), 1,5-pentanediyl-bis(tri-n-butylammonium)di(5-phenyltetrazolate) (**2**) and 1,6-hexanediyl-bis(tri-n-butylammonium)di(5-phenyltetrazolate) (**3**): 26.65 mmol, 14.61 mmol respectively of already prepared 1,4-butanediyl-bis(tri-n-butylammonium)dibromide and 1,5-pentanediyl-bis(tri-n-butylammonium)dibromide was dissolved in sodium 5-phenyl tetrazolate solution resp. in water and 20.45 mmol of 1,6-hexanediyl-bis(tri-n-butylammonium)dihydroxide was mixed with 40.90 mmol of 5-phenyltetrazolate, both

the reactions of which were allowed to stir for 3-4 hours at a temperature of 60 degrees or overnight at room temperature.

4. Formation of crystals of the prepared dicationic liquid: the ionic liquids 1,2 and 3 were set for crystal formation process by vapour diffusion techniques and or cold crystallization techniques. Thin needle-like crystals for 2 were obtained by cold crystallization in ethylacetate whereas, vapour diffusion with mixed solvent system yielded crystals for 1 and 3.

5. Further synthesis of different functionalised tetrazoles for ionic liquid formation is underway.

6. Attempt at synthesising a deuterated sample of a quaternary phosphonium salt was taken using 10% Pt/C with a mixed solvent system using D_2O. The parameters needs to be modified for desired yields of the salt.

Conclusions and future work

1. Synthesis of ionic liquids and LCST behaviour of them in water has been initiated and study of systems containing (i) anion modification and (ii) cation modification, both demonstrating how critical temperature and hydrophilicity can be modified.

2. Assessment of the 'pre-requisites' for an IL to behave as an efficient draw solute for FO, like the osmotic pressure, viscosity, and development of strategies to implement these within materials (for example, addition of hydrophilic groups to enhance water flux, etc) along with measuring the water osmotic pressures.

3. Understand molecular interactions of ionic liquids using simulation studies will be carried out.

4. Preparing samples for neutron scattering experiments at ISIS are underway.

QUILL Quarterly Report

November 2022 – January 2023

Name:	David McAreavey		
Supervisor(s):	Dr Stephen Glover, Dr Oana Istrate and Prof Peter Nockemann		
Position:	PhD student		
Start date:	1st October 2021	**Anticipated end date:**	31st March 2025
Funding body:	Department for the Economy		

Design and Development of an Effective and Interconnected Smart Fire Suppression System for Lithium-ion Batteries in Electric Vehicles

Background

As many countries around the world begin to implement their plans to ban the sale of new petrol and diesel vehicles in the coming decades, there is a clear shift occurring towards electrification of transportation. However, there are several challenges that should be addressed if mass adoption of these vehicles is to be successful. Chiefly among which are the needs to extend range and improve battery safety. Depending on the sources used it can be argued that EVs do have a good battery safety record and the number of electric vehicle fires that occur are relatively low. Tesla's 2020 vehicle safety report claims that one of their vehicles is almost ten times less likely to be involved in a vehicle fire, than the average vehicle on the road in America per mile driven, based on data from the national Fire Protection Association and US Department of Transportation. Contrary to this, in London in 2019 based on data from the London Fire Brigade the incident rate when adjusted for the number of EVs and IC vehicles on the road is more than twice as high for EVs. Regardless of the exact frequency, due to the nature of these thermal events they can often initiate thermal runaway, meaning that it is extremely difficult to extinguish as well as having the potential to burn both hotter and longer than a typical IC vehicle fire. The primary concern is of course for the safety of the occupants of the vehicle and the potential danger to their health. Additionally, an EV has the potential to ignite in scenarios where it may initially go unnoticed, usually if an IC vehicle ignites it will do so in use as this is when the highest temperatures are experienced. EVs on the other hand can ignite under circumstances such as when charging. This means that the thermal runaway process may go unnoticed for some time as well as likely being close to a home or garage, causing significant property damage.

An additional concern surrounding the adoption of EVs is the level of media attention that EV fires receive. Despite being relatively infrequent especially due to the low total market share, the negative publicity generated hinders the adoption of these vehicles. As well as causing the loss of resources that were originally carbon intensive to produce.

Objective of this work

The ultimate goal is to develop a fire suppression and thermal management system that can be realistically employed in a vehicle. This work may only achieve a step in this development for such a suppression system. It is vital to consider that such a system must be compatible

with thermal management systems, as the implementation of a fire suppression system without an appropriate thermal management system essentially renders the vehicle useless. This means that a vehicle has the ability to keep the cells within its pack in the optimal temperature range, promoting longevity. As well as having a sufficient suppression system that is capable of preventing the propagation of thermal runaway between cells in the event of a fault or road traffic collision.

Progress to date

Since November there has been consistent focus on delivering a model that can be used to predict the outcome of a runaway event based on the cooling and propagation system employed. As mentioned in previous reports there is significant complexity in deciphering where the limits of the present work lies. The model that is still being developed and refined employs fundamental equations set out by Hatchard et al in 2001 for the kinetics of a cell in decomposition, while these equations underpredict the peak temperature experienced by a cell in runaway, they do predict the point of initiation well. As such the propagation prediction can be made using these equations with the understanding that the peak temperature is incorrect. The triggering of these runaway events even in modelling is also an area that is hard to find a cohesive approach in the literature. As such the approach for this work uses calorimetry data for total heat output mapped to a bell curve which will allow the profiles to be tweaked and modified to look at the critical parameters.

Alongside this the MATLAB models developed are being validated against literature at steps throughout the development. The intention is to produce a conference paper with the model developed. The preliminary results obtained from the model give a more optimistic prediction for the use of PCMs than the previously used implementation. In that case a temperature profile was used and it was expected that this would overpredict the cell spacing that would be required. Previously a spacing of 5mm was required to avoid runaway propagation where as with this refined model with a cell energy content of 45kJ of electrical energy for an 18650 cell a spacing of between 2 and 3mm would be sufficient when considering a pure paraffin but this assuming the combustion of the paraffin itself could be avoided with the use of fire retardant additives.

Conclusions and future work

A model that can be used to assess the benefit of different cooling systems has been mostly completed, there is work underway to produce a paper based on this work with continued refinement ongoing. The main focus of this paper is intended to be the weight volume and mass implications of these PCM systems.

QUILL Quarterly Report

November 2022 – January 2023

Name:	Sam McCalmont		
Supervisor(s):	Dr Leila Moura, Prof John Holbrey and Prof Margarida Costa Gomes		
Position:	PhD		
Start date:	Jan 2020	**Anticipated end date:**	July 2023
Funding body:	EPSRC Doctoral Training Partnership		

Chemisorbent Materials for Olefin and Paraffin Separation

Background

Separation of light olefins from their paraffin counterparts have been described as one of the seven chemical separations to change the world.[1] Global annual production of light olefins exceeds 200 million tons, about 30 kg for each person on the planet. The current method for their separation is cryogenic distillation, one of the most energy-intensive processes in the industry. Alternative methods can focus on the olefin being selectively captured either through a physical interaction (physisorption) or chemical reaction (chemisorption).

One class of alternative sorbents are ionic liquids (ILs). However, so far, IL physisorbents have not demonstrated sufficient efficiency in either selectivity or capacity to compete with current technologies.[2] Complexation of ethylene through its double bond with silver and copper ions has been used in the literature for chemical separation of olefins and paraffins. However, other components of raw gas feeds, such as acetylene, can react with the silver and become explosive. This has prevented the uptake of these materials into large scale processes.

Objective of this work

To develop and test new chemisorbent materials for the separation of light olefins and paraffins; to achieve high capacity combined with selectivity for the selected materials. To investigate, and rationalise, selectivity and capacities of chemisorbent based on measurement of gas solubility and partitioning from model industrial gas stream compositions and conditions.

Progress to date

In summary, for the last few months of the PhD program, the time has been divided between two main projects. Both papers focus on the use of nitrile groups in ionic liquids as their inclusion has shown to increase the separation potential of ethylene and ethane, why this exactly is, is not known.[3] One will be focusing on nitrile groups in the anion of the ionic liquid (paper A) and one will focus on the nitrile groups present in the cation (paper B). Paper B will include the study of mixtures of different salts (inorganic/organic) to study the influence of the mixing for the solubility of ethylene and ultimately the separation. This is where the work completed in Lyon will be added to. This paper may include the work involving ionic liquids plus metal salts which will be added keeping in theme with the mixtures. For both paper A

and B, molecular dynamic studies are being investigated by a collaboration project within the School of Mathematics and Physics in Queen's University Belfast.

Paper A:
This paper will focus on including the nitrile functional group in the anion while keeping a constant cation. The common cation chosen will be $[C_4C_1Im]^+$ cation. The anions chosen (increasing order of nitrile group content) are thiocyanate $[SCN]^-$, dicyanamide $[DCA]^-$, tricyanomethanide $[TCM]^-$, and tetracyanoborate $[TCB]^-$. Currently no viable source of tetracyanoborate has been found, and since no viable option is available, the molecular dynamic simulations can provide some information on the use of $[TCB]^-$ for the separation of ethylene and ethane, and if it could be beneficial to pursue and justify the economic cost.

The solubility of ethylene and ethane in the ionic liquids have been determined so far *via* the screening method. All three ionic liquids present lower absorption capacity for the uptake of ethane and ethylene than $[C_4C_1Im][NTf_2]$, matching the literature data on nitrile based ionic liquids. The nitrile based ionic liquids have preferential solubility to ethylene compared to that of $[C_4C_1Im][NTf_2]$. With the screening method, the selectivity towards ethylene for $[C_4C_1Im][NTf_2]$ was determined as ~1.4:1 (similar to literature) compared to the nitrile ionic liquids which contain higher selectivity. This is the reasoning behind the use of the nitrile based ionic liquids. These selectivities for the ionic liquids are shown in Figure 2. $[C_4C_1Im][DCA]$ selectivity towards ethylene is similar to literature.[3]

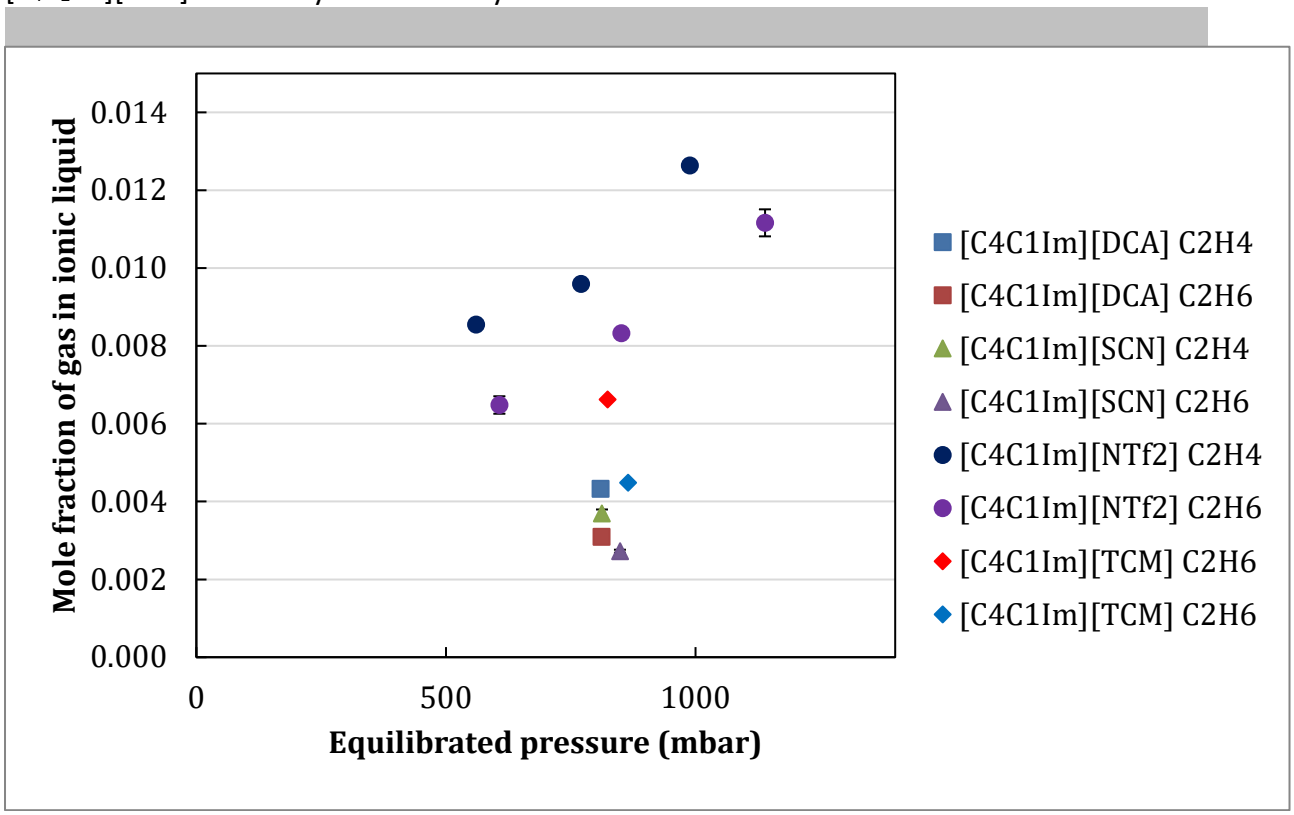

Figure 1 - The solubility of ethylene and ethane in $[C_4C_1Im][SCN]$, $[C_4C_1Im][DCA]$, and $[C_4C_1Im][TCM]$ compared against that of $[C_4C_1Im][NTf_2]$.

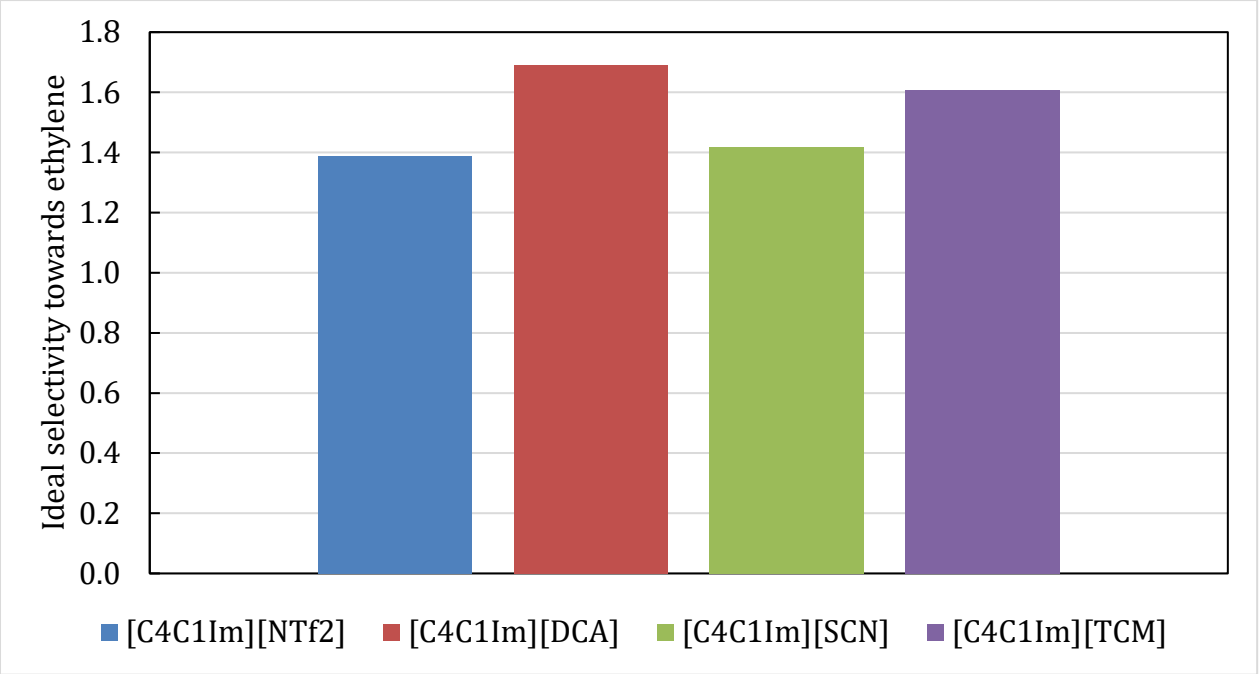

Figure 2 - Selectivity towards ethylene from ethane for the ionic liquids from Paper A. Corresponding error still being determined.

Paper B:

The following cyanopyridinium ionic liquids will be included in this paper. The butyl-4-cyanopyridinium bis(trifluoromethylsulfonyl)imide ($[C_4{}^4CNPy][NTf_2]$) and butyl-3-cyanopyridinium bis(trifluoromethylsulfonyl)imide ($[C_4{}^3CNPy][NTf_2]$), and a 50:50% molar mixture of butyl-4-cyanopyridinium bis(trifluoromethylsulfonyl)imide ($[C_4{}^4CNPy][NTf_2]$) : 1-butyl-4-imidiazolium bis(trifluoromethylsulfonyl)imide ($[C_4C_1Im][NTf_2]$) are currently being studied for ethylene and ethane solubility. The purpose of using the mixture is to promote the use of the $[C_4C_1Im][NTf_2]$ as a dilutant and perhaps promoting the solubility of ethylene and ethane. This could perhaps promote more physisorption to occur, or perhaps allow for the stronger interactions to occur around the $[C_4{}^4CNPy]^+$ when it is in a more free environment. The solubility of the gases (ethylene, ethane and mixed ethylene/ethane) is ongoing and will finish at the end of February 2023. This work will be presented during two upcoming conferences: ChemEngDayUk2023 (Belfast, UK) and COIL9 (Lyon, France).

The isothermal titration nanocalorimetry data of mixing different compositions of butyl-4-cyanopyridinium bis(trifluoromethylsulfonyl)imide ($[C_4{}^4CNPy][NTf_2]$) : 1-butyl-4-imidiazolium bis(trifluoromethylsulfonyl)imide ($[C_4C_1Im][NTf_2]$) have been collected and this was collected during the research visit in Lyon will be added to this paper (as described during the last quarterly report).

A summary from this work showed that the enthalpy of mixing of the two ionic liquids was only slightly positive, suggesting that the ionic liquids mixed ideally with no new interaction between them. Work conducted before involving the mixing of metal salts and $[C_4C_1Im][NTf_2]$ using the screening method will be included in this section (this data again described before during a previous quarterly report).

Paper C:
Title: “Insights into the absorption of hydrocarbon gases in phosphorous-containing ionic liquids”. The paper has been accepted to the Journal of Physical Chemistry B, and currently the corrections from the reviewers have just been completed. This was focused on during January. This paper focuses on the separation of olefins and paraffins (specifically ethylene/ethane and propylene/propane).

Conclusions and future work

For both papers, the characterisation and solubility data are being collected, and will be collected during the last months of the PhD project. During this coming quarter, the groundwork for both papers will be written, and the data and results will be added as they are ready.

References

1. D. S. Sholl and R. P. Lively, *Nature*, 2016, **532**, 435–437.
2. L. Moura, C. C. Santini and M. F. Costa Gomes, *Oil Gas Sci. Technol. – Rev. d’IFP Energies Nouv.*, 2016, **71**, 23.
3. L. Moura, W. Darwich, C. C. Santini and M. F. Costa Gomes, *Chem. Eng. J.*, 2015, **280**, 755–762.

QUILL Quarterly Report

November 2022 – January 2023

Name:	Emma McCrea		
Supervisor(s):	Prof Małgorzata Swadzba-Kwasny and Prof John Holbrey		
Position:	PhD student		
Start date:	01/09/21	**Anticipated end date:**	01/09/24
Funding body:	Engineering and Physical Sciences Research Council (EPSRC)		

Valorisation of Waste Polyolefin Plastics Using Lewis Acidic Ionic Liquids

Background

Waste polyalphaolefin plastic can be processed using pyrolysis to produce a mixture containing a wide distribution of alphaolefin/paraffin products. This mixture can be used to generate waxes, a higher value product and a low value naphtha fraction. Using the naphtha fraction from the waste polyolefin pyrolysis (C8-C20) and a Lewis acidic ionic liquid, the oligomerisation of 1-olefins to base oil is performed. The resulting base oil should have key physical properties to that of synthetic Group IV base oils including high viscosity index (>120) combined with low kinematic viscosities (Kv_{100} = 4 cSt or 6 cSt). Producing both waxes and base oil increases the overall economic feasibility of the process which adopting a circular economy cradle to cradle approach.

Borenium ionic liquids with the general formula $[BCl_2(L)][Al_2Cl_7]$ (L = pyridine or picoline) and liquid coordination complexes based on $AlCl_3$, L-$AlCl_3$ (L = Urea or $P_{888}O$) are selected as they have high Lewis acidities and synthesised from readily available and chemicals.

Using waste polyalphaolefin plastic as a feedstock poses challenges as it highly contaminated. The recycled feedstock must be purified before oligomerisation is performed. Additives and liquid-liquid extraction are selected based on the ability to remove impurities and analysed by XRF and ^{13}C NMR.

Objective of this work

In this project, the goal is to convert 1-olefins in the naphtha fraction to lubricant base oil using liquid coordination complexes and borenium ionic liquids. The analysis of product distributions (by SimDist GC) and physical parameters are then compared to the industry standard. Before the oligomerisation can take place the impurities in the feedstock must first be removed. Without the removal of impurities, the liquid coordination complexes and borenium ionic liquids fail to oligomerise 1-olefins. This is an area of focus on this project to find sustainable method to remove impurities.

Progress to date

In the previous report, methods to reduce the level of impurities by liquid-liquid extraction and deep eutectic solvents failed to remove impurities to a level that enabled the liquid coordination complex and borenium ionic liquid catalyst to perform oligomerisation.

Feedstock impurities

A new batch of washed polyalphaolefin plastic was obtained and XRF analysis showed lower levels of impurities than the original feedstock. After distillation and washing (100 ml x3 water) the impurities were all below 35 ppm. (Fig. 1-4)

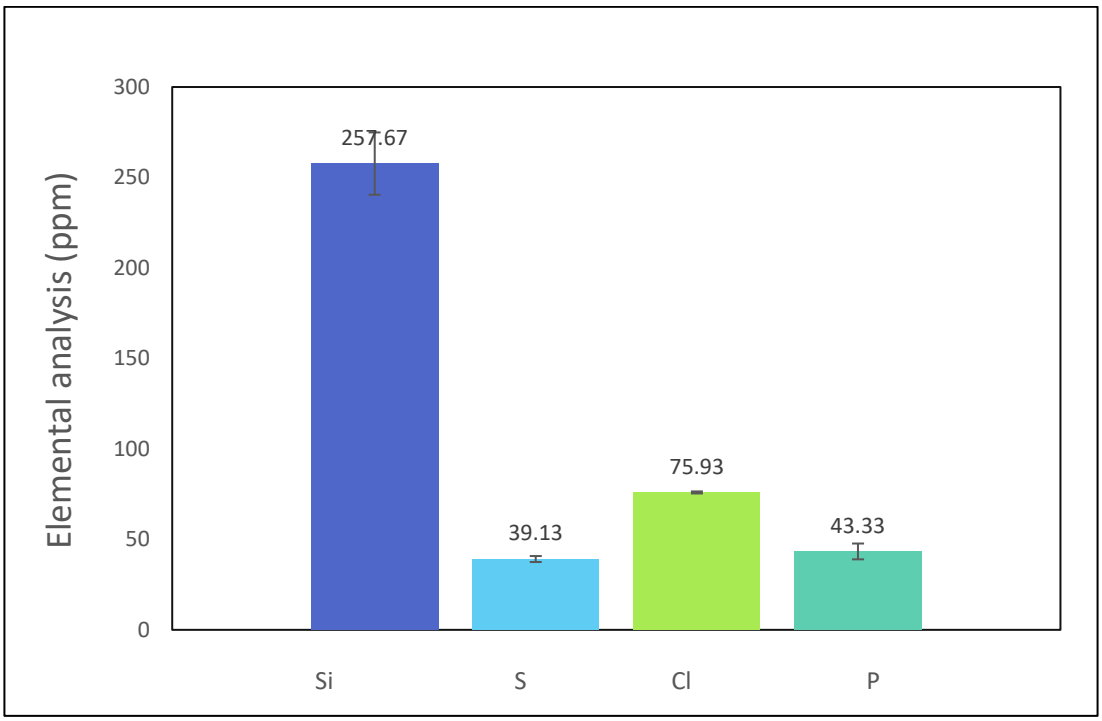

Figure 1 - XRF analysis of original feedstock

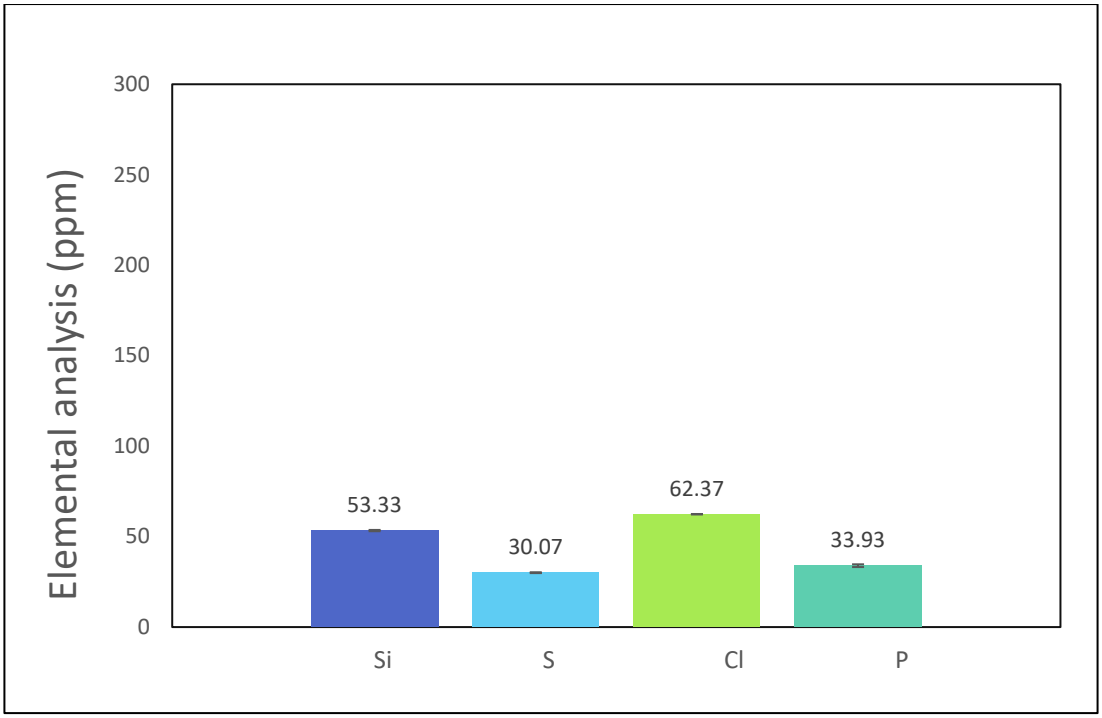

Figure 2 - XRF analysis of new crude feedstock

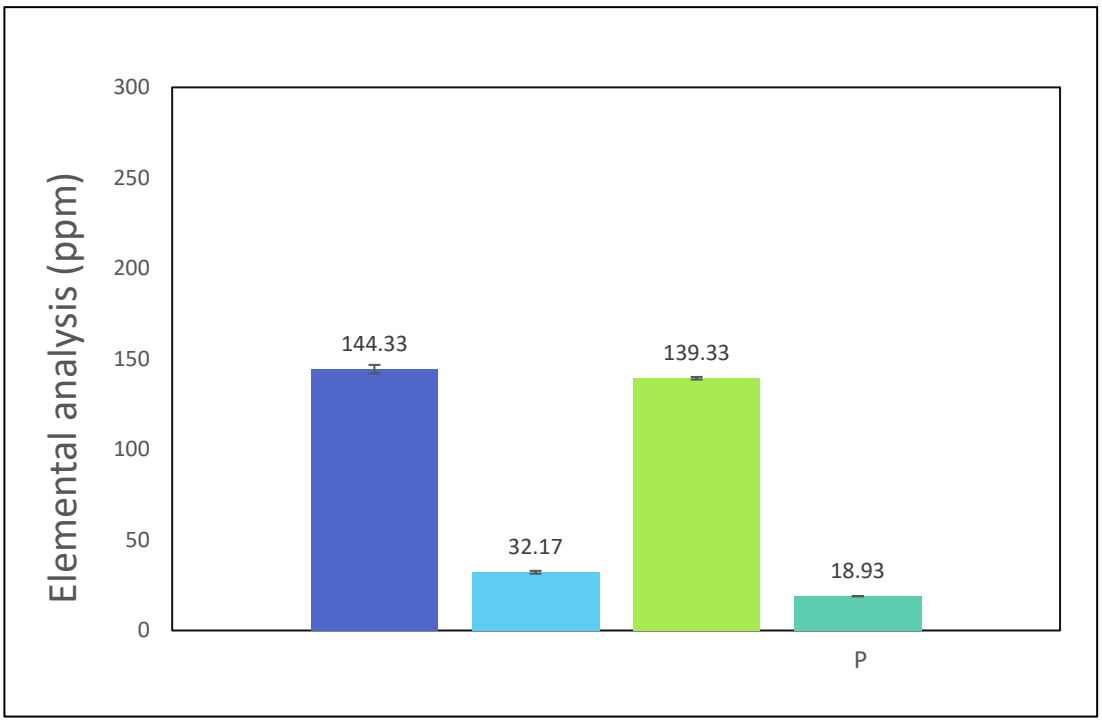

Figure 3 - XRF analysis of distilled feedstock

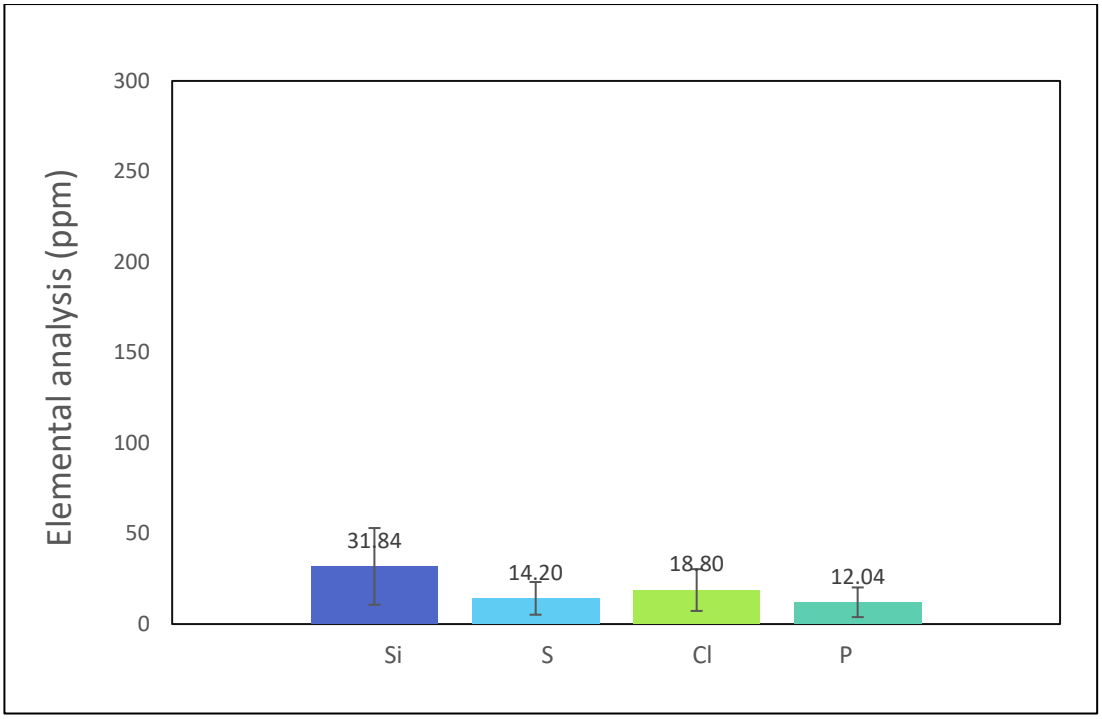

Figure 4 - XRF analysis of washed feedstock

Oligomerisation

Liquid coordination complexes and borenium ionic liquids were prepared in the glovebox. Experiments were carried out in computer-controlled H.E.L reactors with feedstock under argon. LCCs/IL is added dropwise via a syringe and quenched with water. The product was dissolved in cyclohexane (100 mg cm^{-3}), dried over magnesium sulphate, filtered and analysed according to ASTM D7500. Results are shown in fig. 5 and 6.

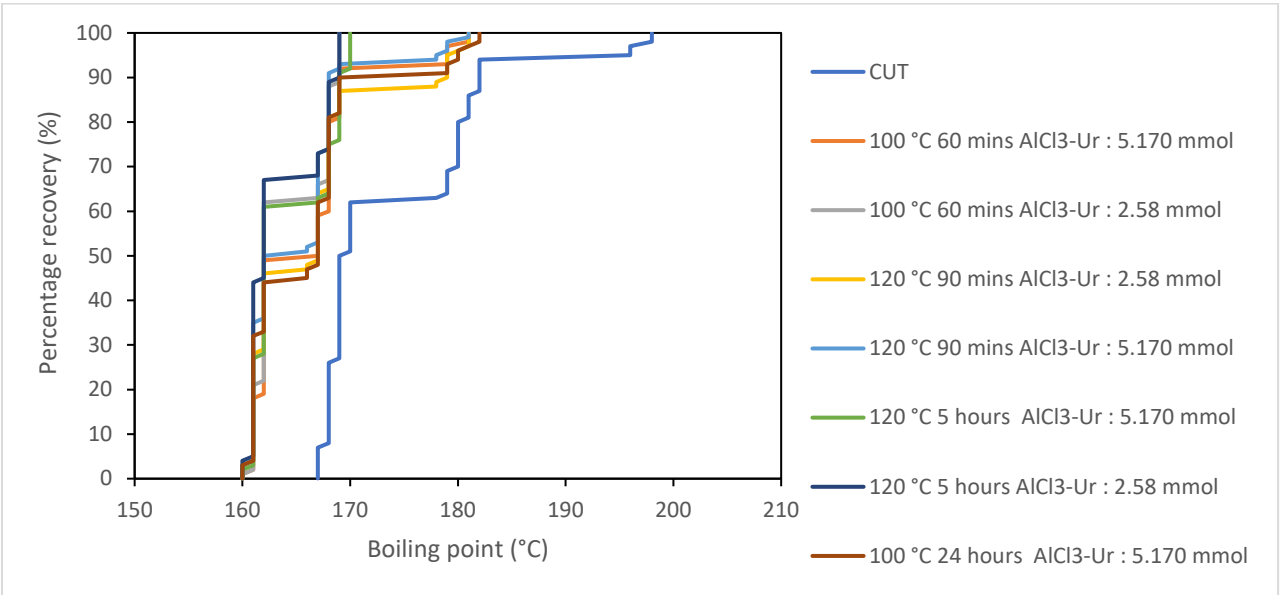

Figure 5 - Percentage recovery (%) using liquid coordination complex.

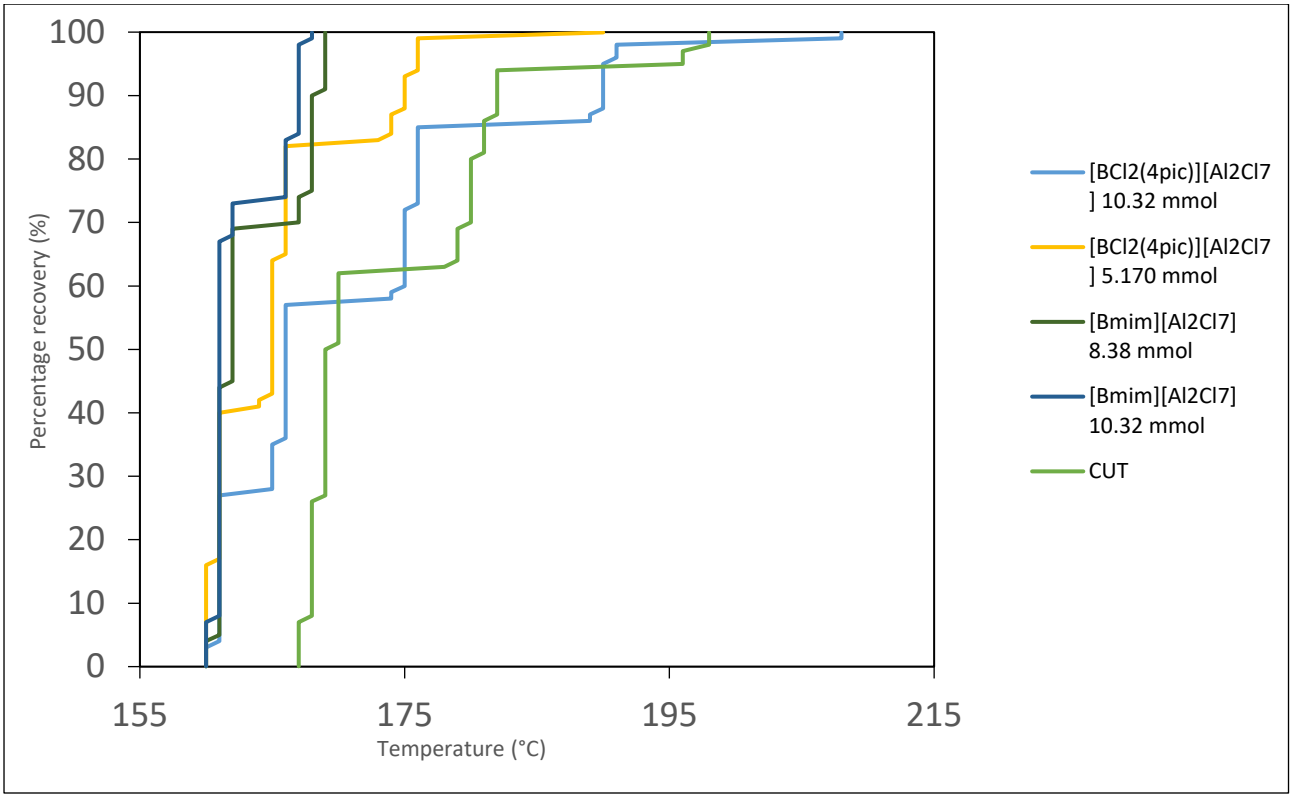

Figure 6 - Percentage recovery (%) using ionic liquids.

	CUT	**$[BCl_2(4pic)][Al_2Cl_7]$**	**$[BCl_2(4pic)][Al_2Cl_7]$**	**$[BCl_2(4pic)][Al_2Cl_7]$**	**$[Bmim][Al_2Cl_7]$**
Fractions	Recovery (%)	10.32 mmol	5.170 mmol	5.170 mmol	10.32 mmol
>C9	0	0	0	0	0
C9	62.4	57.6	87.1	100	100
C10	33.7	40.6	12.9	0	0
C11	3.8	1.7	0	0	0
C12	0	0	0	0	0
C14	0	0	0	0	0
C15	0	0	0	0	0
C16-20	0	0	0	0	0
C20-C50	0.1	0	0	0	0
C50-C100	0	0	0	0	0
		40 °C	40 °C	40 °C	40 °C
		3 hours	3 hours	3 hours	3 hours

Table 1 - Percentage recovery of fractions

The new batch of feedstock with lower impurities allowed a reaction to occur unlike the previous feedstock were the product distribution remained unchanged after the addition of the Lewis acidic ionic liquid catalyst. The product recovery showed that the feedstock was cracked into smaller monomers rather than oligomerised which wasn't expected. The fractions produced are within the jet fuel range.

Conclusions and future work

The borenium ionic liquids and liquid coordination complexes with the waste plastic feedstock shifts the product distribution toward the lighter fraction. The original thought was that oligomerisation would take place shifting product distribution to the heavier fraction. This provides an alternative area of focus into jet fuels.

Next steps, analysis of the products of the reaction with Simdis GC and GC-MS using jet fuel methods. Then the alkylation of benzene with the waste plastic feedstock and sulfonation.

QUILL Quarterly Report

November 2022 – January 2023

Name:	Anne McGrogan		
Supervisor(s):	Prof Gosia Swadzba-Kwasny		
Position:	PhD		
Start date:	01/10/2019	**Anticipated end date:**	31/03/2023
Funding body:	EPSRC		

Liquid-liquid Transition in Phosphonium Ionic Liquids

Background

This project was a collaboration with Zaneta Wojnarowska from University of Silesia, Katowice. The work investigates first-order liquid-liquid transition (LLT) in a series of ionic liquids containing trihexyl(tetradecyl)phosphonium cation $[P_{66614}]^+$ and anions of different sizes and shapes, providing an insight into the structure-property relationships governing LLT. My involvement in this work was the synthesis of some ionic liquids. $[P_{66614}][NTf_2]$ exhibits a clear LLT and this ionic liquid was selected to study its liquid structure above and below LLT by neutron scattering. This work will describe the synthesis of deuterated $[P_{66614}][NTf_2]$ and its liquid structure by neuron scattering and analysis of the data using DISSOLVE software.

When isotropic liquid is cooled below its melting point, it either crystallises, or enters a metastable supercooled state, which turns into a non-equilibrium amorphous phase (glass). However, a few single-component materials exhibit yet another behaviour, undergoing a first-order liquid-liquid transition (LLT). LLTs separate fluids of different local structures, density and thermodynamic properties. They have been detected in various media, from atomic elements (sulfur, phosphorus,[1] silicon,[2,3] carbon[4]) to molten oxides.[5,6,7] Only four room temperature molecular liquids exhibit LLT: water,[8,9] triphenyl phosphate,[10,11,12] *n*-butanol[10] and D-mannitol.[13] Nevertheless, LLT in these systems remains controversial, since it occurs in the supercooled state capable of cold crystallisation.[14] Furthermore, very little is known about the effect of molecular packing on LLT, except for a few simple cases.[15,16] Consequently, critical factors inducing such a transition are unclear. The first evidence of LLT in aprotic ionic liquids (ILs) was reported in 2021 for trihexyl(tetradecyl)phosphonium tetrahydroborate, $[P_{666,14}][BH_4]$.[17] Upon the transition, the IL was reported to undergo enhanced ordering of the alkyl chains in the nonpolar domains, as inferred from calorimetric, XRD and IR spectroscopy data. This work inspired our own systematic investigation into LLTs in $[P_{66614}]^+$ ionic liquids based on six anions: $[BF_4]^-$, $[SCN]^-$, $[TAU]^-$, $[TFSI]^-$ $[BOB]^-$ and $[TCM]^-$. $[P_{66614}][BF_4]$ crystallised from supercooled melt, $[P_{66614}][BOB]$ underwent a glass transition, and the four remaining samples exhibited LLT in a differential scanning calorimetry (DSC) experiment. In addition to calorimetric proof of LLT *via* DSC, the phase change was detected by the measurement of conductivity relaxation times, both under isobaric cooling and under isothermal compression up to 500 MPa. This work has been published in *Nature Commun.*[18]

The next stage of this work is to synthesise deuterated $[P_{66614}][NTf_2]$ to study its structure by neutron scattering. Neutron diffraction is a highly effective technique for observing structures

in the liquid state. Hydrogen/deuterium substitution is a crucial and very powerful tool in neutron diffraction experiments. While X-ray scattering of each atom is dependent on the atomic number (Z), in neutron scattering the incident beam interacts with the nucleus of the atoms. Owing to the differences in the sign of the coherent scattering between 1H and 2H (-3.74 fm and 6.67 fm), the comparison of the data recorded from the isotopically substituted systems is a very useful tool in computer simulations.[19] Furthermore, although 1H scatters best, it provides a lot of inelastic scattering which detracts from overall data quality. Therefore, for neutron scattering measurements, it is most beneficial to study both protiated and deuterated analogues of the species of interest, in addition to equimolar mixtures for best data quality.

Objective of this work

To synthesise deuterated $[P_{66614}][NTf_2]$ and to study its liquid structure above and below LLT by neutron scattering using DISSOLVE software.

Progress to date

The synthesis of deuterated $[P_{66614}][NTf_2]$ is reported, following a procedure adapted from Rob Atkin *et al.*[20]

Synthesis of 1-tetradecylchloride-d_{29}

Tetradecanol was synthesised at the Deuteration Facility at ISIS Neutron and Muon Source, STFC Rutherford Appleton Laboratory in Oxfordshire, UK.

13.93 g (0.117 mol) of thionyl chloride was placed in a 2-necked flask equipped with condenser and pressure equalising dropping funnel, which were both fitted with calcium chloride guard tubes. 9.5 g of tetradecanol-d_{29} was placed in the pressure equalising dropping funnel and added slowly with stirring. Evolution of heat and SO_2 evolved. When all the alcohol was added, the mixture was refluxed for 3 hours. The excess of thionyl chloride was then distilled (78-80 °C), and the crude 1-tetradecylchloride at 98 °C and 0.5 mbar. This was then washed with D_2O, 10% sodium carbonate solution and twice with D_2O. Then, dried with anhydrous calcium chloride and distilled again.

^{1}H NMR ($CDCl_3$) residual protons δ 0.88 (m), 1.23 (m), 1.38 (m), 1.58 (m), 1.75 (m), 3.52 (m)
^{2}H NMR ($CDCl_3$) δ 0.82(s, 3D), 1.19 (m, 19D), 1.35 (m, 2.5D), 1.70 (m, 2D), 3.48 (m, 2.0D)
^{13}C NMR ($CDCl_3$) δ 13.1 (m), 21.4 (m), 25.8 (m), 28.4 (m), 30.04 (m), 31.8 (m). 44.2 (m)

Synthesis of trihexyltetradecylphosphonium bis(trifluoromethylsulfonyl)amide-d_{68}

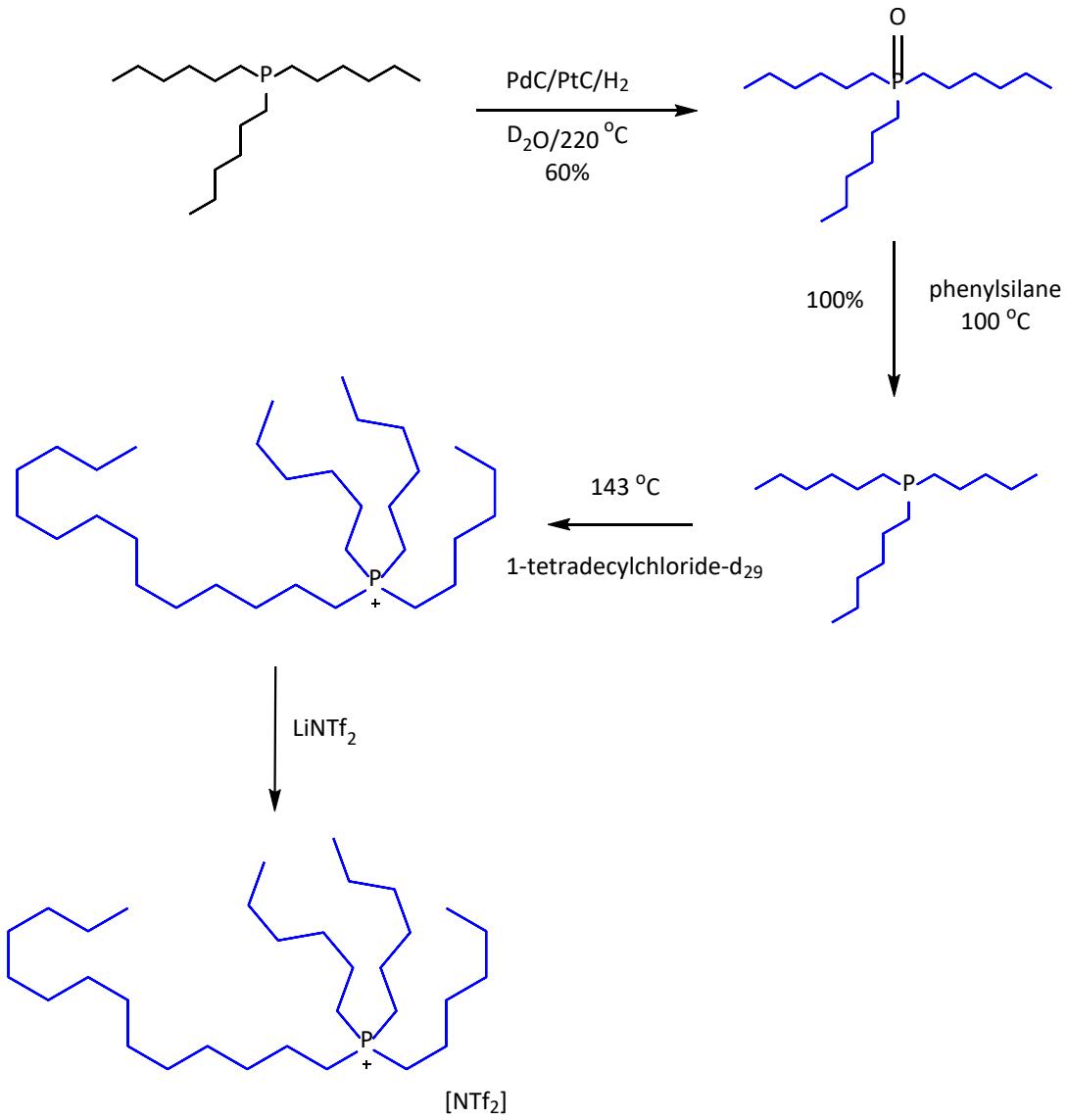

Scheme 1 - Synthesis of trihexyltetradecylphosphonium bis(trifluoromethylsulfonyl)amide-d_{68}

Deuteration of trihexyphosphine oxide-d_{39}

A mixture of trihexylphosphine (3.5 g, 0.00987 mol), 10% Pt/C catalyst (0.75 g), and 10% Pd/C catalyst (0.75 g) in D_2O (65 mL) was stirred under N_2 bubbling for 2 min followed by H_2 bubbling for 2 min at room temperature. The reaction mixture was heated at 220 °C for 1 day. After cooling, the reaction mixture was diluted with dichloromethane, filtered through Celite, washed with dichloromethane and then the aqueous phase was extracted with dichloromethane (3 x 50 mL). The combined extracts were dried over $MgSO_4$ and then evaporated to give deuterated trihexylphosphine oxide-d_{39} as a white solid (1.7 g, 49% yield).

^{1}H NMR ($CDCl_3$) residual protons δ 0.81 (m), 0.87 (m), 1.23 (m), 1.29)m), 1.32 (m), 1.49 (m), 1.62 (m).
^{2}H NMR ($CDCl_3$) δ 0.78(m, 6.7D), 1.18 (m, 8.2D), 1.28 (m, 4.0D), 1.44 (m, 4D), 1.58 (m, 3.57D)

^{13}C NMR ($CDCl_3$) δ 12.7 (m), 21.1 (m), 26.9 (m), 29.7 (m).
^{31}P NMR ($CDCl_3$) δ 50.
ESI-MS [M+Na] m/z 364, isotopic distribution with 93% D level, *d*33 1.5%, *d*34 10.5%, *d*35 13.5%, *d*36 17.7%, *d*37 21.0%, *d*38 21.6%, *d*39 14.2%

Synthesis of deuterated trihexylphosphine-d_{39}
A solution of trihexylphosphine oxide-d_{39} (4.5 g, 0.0149 mmol) in phenylsilane (6 mL) was heated to 100 °C under argon overnight. The reaction was monitored by ^{31}P NMR in degassed $CDCl_3$ through the disappearance of the starting material peak at 50.8 ppm and the appearance of trihexylphosphine peak at -33.65 ppm.
Phenylsilane was removed under reduced pressure to give pale yellow residue, which is used in the next step without further purification.

Synthesis of deuterated trihexyltetradecylphosphine chloride-d_{68}
Trihexylphosphine-d_{39} (4.5 g, 0.0127 mol) and tetradecylchloride-d_{29} (4.32 g, 0.0165 mol) neat were heated to 140 °C in a sealed tube in the glovebox. The temperature was maintained at 143 ºC for 24 hrs. The progress of the reaction was monitored by ^{31}P NMR spectroscopy in $CDCl_3$ (^{31}P peak at at -33.65 ppm disappeared to give a peak at 32 ppm.

^{1}H NMR ($CDCl_3$) residual protons δ 0.88 (m), 0.91 (m), 1.21 (m), 1.27)m), 1.34 (m), 1.44 (m), 1.49 (m), 1.77 (m), 2.16 (m), 2.20 (m).
^{2}H NMR ($CDCl_3$) δ 0.78 (m, 6.7D), 1.18 (m, 8.2D), 1.28 (m, 4.0D), 1.44 (m, 4D), 1.58 (m, 3.57D), 2.14 (3.0D).
^{13}C NMR ($CDCl_3$) δ 12.7 (m), 21.1 (m), 26.9 (m), 29.7 (m).
^{31}P NMR ($CDCl_3$) δ 32.
ESI-MS [M+1] m/z 552. Isotopic distribution 96% D level, *d*63 6.7%, *d*64 14.8%, *d*65 23.0%, *d*66 25.9%, *d*67 20.3%, *d*68 9.2%.

Synthesis of deuterated trihexyltetradecylphosphonium bis(trifluoromethylsulfonyl)amide-d_{68}

Trihexyl(tetradecyl)phosphonium chloride [$P_{666,14}$][Cl] (0.010 mol eq.) was dissolved in hexane and Li[TFSI] was dissolved in D_2O, combined in a round-bottomed flask, and left to react (1 h, RT, 600 rpm). The organic layer was separated and washed with D_2O. Hexane was removed and the ionic liquid was dried under high vacuum (12 h, 70 °C, 10^{-2} mbar).

^{1}H NMR ($CDCl_3$) residual protons δ 0.88 (m), 0.91 (m), 1.21 (m), 1.27)m), 1.34 (m), 1.44 (m), 1.49 (m), 1.77 (m), 2.16 (m), 2.20 (m).
^{2}H NMR ($CDCl_3$) δ 0.78 (m, 6.7D), 1.18 (m, 8.2D), 1.28 (m, 4.0D), 1.44 (m, 4D), 1.58 (m, 3.57D), 2.14 (3.0D).
^{13}C NMR ($CDCl_3$) δ 12.7 (m), 21.1 (m), 26.9 (m), 29.7 (m).
^{31}P NMR ($CDCl_3$) δ 32.
^{19}F NMR ($CDCl_3$) δ -79
ESI-MS [M+1] m/z 552. Isotopic distribution 96% D level, *d*63 6.7%, *d*64 14.8%, *d*65 23.0%, *d*66 25.9%, *d*67 20.3%, *d*68 9.2%.

Neutron scattering data were collected using the NIMROD (Near and InterMediate Range Order Diffractometer) instrument at the ISIS pulsed neutron and muon source, Rutherford Appleton Laboratory, UK. Data was collected for three samples: $[P_{66614}][NTf_2]$, $[d_{68}\text{-}P_{66614}][NTf_2]$ and their equimolar mixture. Each sample was measured at -43 and -93 °C, in TiZr cans. Prolonged storage at -93 °C could result in spontaneous crystallisation, but from preliminary experiments it was known, that samples can be held at this temperature for at least 1 h without crystallising. Data was recorded for 3 h at -93 °C. The data was collected in 10 min runs as an additional precaution to minimise the risk of recording data on the crystalline phase. The data was also recorded for 3 h at -43 °C and data was also collected while heating. To record data at these temperatures, the experiment required the use of the closed cycle refrigerator (CCR). Standard corrections and normalisations were applied to the data using the Gudrun software.[21] Data was collected on the empty NIMROD instrument at the two temperatures and with an empty TiZr can at both temperatures.

Data was firstly collected for the protiated $[P_{66614}][NTf_2]$ sample. As the data was collected at the lower temperature, it was analysed to make sure that crystallisation was not occurring. The presence of bragg peaks would indicate crystallisation. Crystallisation of this sample did not occur, and all data was collected successfully. However, when analysing the data collected at -43 °C for the $[d_{68}\text{-}P_{66614}][NTf_2]$ sample, bragg peaks were present. Clearly, the deuterated ionic liquid has different phase behaviour compared to the protiated version. The equimolar mixture also showed similar behaviour, with crystallisation observed at -32 °C. Another mixture was tested, 75% $[P_{66614}][NTf_2]$ and 25% $[d_{68}\text{-}P_{66614}][NTf_2]$ which also showed similar behaviour. This was very surprising.

Room temperature neutron scattering data was then collected for the three samples: $[P_{66614}][NTf_2]$, $[d_{68}\text{-}P_{66614}][NTf_2]$ and the 75:25 $[P_{66614}][NTf_2]$:$[d_{68}\text{-}P_{66614}][NTf_2]$ mixture. The liquid structure of $[P_{66614}][NTf_2]$ has never been studied before using neutron scattering. An initial model for the data has been built in Dissolve and is currently being analysed.

References

1. Y. Katayama, T. Mizutani, W. Utsumi and O. Shimomura, 2000, **403**, 1998–2001.
2. V. V. Vasisht and S. Sastry, *Adv. Chem. Phys.*, 2013, **152**, 463–517.
3. D. J. Superconductivity, R. D. M. Dekker, N. York, I. Saika-voivod, P. H. Poole and F. Sciortino, 2001, **412**, 1–4.
4. J. N. Glosli and F. H. Ree, *Phys. Rev. Lett.*, 1999, **82**, 4659–4662.
5. W. Xu, M. T. Sandor, Y. Yu, H. B. Ke, H. P. Zhang, M. Z. Li, W. H. Wang, L. Liu and Y. Wu, *Nat. Commun.*, 2015, **6**, 1–9.
6. G. N. Greaves, M. C. Wilding, S. Fearn, D. Langstaff, F. Kargl, S. Cox, Q. Vu Van, O. Majérus, C. J. Benmore, R. Weber, C. M. Martin and L. Hennet, *Science (80-.).*, 2008, **322**, 566–570.
7. S. Wei, F. Yang, J. Bednarcik, I. Kaban, O. Shuleshova, A. Meyer and R. Busch, *Nat. Commun.*, , DOI:10.1038/ncomms3083.
8. C. A. Angell and P. D. Bennett, *J. Am. Chem. Soc.*, 1982, **104**, 6304–6309.
9. I. Kaori, M. CT and C. Angell, *Nature*, 1999, **398**, 492–495.
10. R. Kurita and H. Tanaka, *J. Phys. Condens. Matter*, , DOI:10.1088/0953-8984/17/27/L01.

11. R. Kurita and H. Tanaka, *Science (80-.).*, 2004, **306**, 845–848.
12. M. Kobayashi and H. Tanaka, *Nat. Commun.*, 2016, **7**, 1–8.
13. M. Zhu, J. Q. Wang, J. H. Perepezko and L. Yu, *J. Chem. Phys.*, , DOI:10.1063/1.4922543.
14. H. Tanaka, *Phys. Rev. E - Stat. Physics, Plasmas, Fluids, Relat. Interdiscip. Top.*, 2000, **62**, 6968–6976.
15. Q. S. Zeng, Y. Ding, W. L. Mao, W. Yang, S. V. Sinogeikin, J. Shu, H. K. Mao and J. Z. Jiang, *Phys. Rev. Lett.*, 2010, **104**, 1–4.
16. L. Liu, S. H. Chen, A. Faraone, C. W. Yen and C. Y. Mou, *Phys. Rev. Lett.*, 2005, **95**, 1–4.
17. M. A. Harris, T. Kinsey, D. V. Wagle, G. A. Baker and J. Sangoro, *Proc. Natl. Acad. Sci. U. S. A.*, 2021, **118**, 1–6.
18. Z. Wojnarowska, S. Cheng, B. Yao, M. Swadzba-Kwasny, S. McLaughlin, A. McGrogan, Y. Delavoux and M. Paluch, *Nat. Commun.*, 2022, **13**, 1–10.
19. V. F. Sears, *Neutron News*, 1992, **3**, 26–37.
20. P. K. Cooper, H. Li, N. R. Yepuri, A. Nelson, G. B. Webber, A. P. Le Brun, T. A. Darwish, G. G. Warr and R. Atkin, *J. Phys. Chem. C*, 2018, **122**, 24077–24084.
21. A. K. Soper, *GudrunN and GudrunX: Programs for correcting raw neutron and X-ray diffraction data to differential scattering cross section*, 2011.

QUILL Quarterly Report

November 2022 – January 2023

Name:	Shannon McLaughlin		
Supervisor(s):	Professor Gosia Swadźba-Kwaśny		
Position:	PhD Student (3rd year)		
Start date:	October 2020	**Anticipated end date:**	July 2024
Funding body:	Department for the Economy (DoE)		

Lewis Superacidic Ionic Liquids Based on Silicon Cations

Background

The chemistry of Lewis acidic main group cations is of increasing importance, as metal-free catalysis gains interest of the scientific community. One of the longest-standing challenges in main group synthetic chemistry has been the preparation of tricoordinate, tetravalent silicon cations in the condensed phase. Silylium ions are extremely Lewis acidic and have a high electrophilicity, oxophilicity and fluorophilicity, affording unique transformations that cannot be performed by traditional metal catalysts. Recently, synthetic methods to generate stable silylium cations have become more accessible and more effective.

Silylium ions can be categorised as either stabilised or 'free' (Figure 1a). As they are highly reactive, silicon cations are commonly found as species which are stabilised, whereas 'free' silicon cations are extremely rare. The first ever 'free' silylium cation to be isolated was the trimesitylsilylium cation ($(Mes)_3Si^+$) illustrated in Figure 1b.[1] Silylium ions are usually quite a reactive species but the bulky mesityl groups in compound **1** help to shield the silicon centre from attack by large nucleophiles. These steric interactions also prevent the silylium ion reacting with the solvent and the product alkene making it much more stable. The tridurylsilylium cation ($(duryl)Si^+$)[2] was later isolated along with the related species $(C_6Me_5)_3Si^+$.[3] Till date these three compounds are the only examples of 'free' species whose structures have been confirmed by X-ray crystallography.

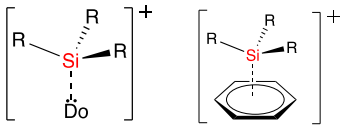

σ-Donor stabilised

π-Donor stabilised

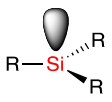

'free' (unstabilised)

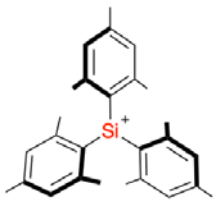

$[B(C_6F_5)]^-$

1

Figure 1 - a) Example structures of stabilised and unstabilised b) Structure of 'free' trimesitylsilylium cation.

Objective

This work reports on the first-ever attempt to prepare and characterise silylium ionic liquids. The first goal of this project is to synthesise the 'free' trimesitylsilylium cation illustrated in Figure 1b.

Progress to date

Synthesis of trimesitylsilane:

Trimesitylsilane was synthesised following the method described by Lappert *et al.*[4] 0.74 g of trimesitylsilane was synthesised (white crystals shown in Figure 2). A second batch of trimesitylsilylium was synthesised to increase the yield. ^{1}H, ^{13}C and ^{29}Si NMR spectra for trimesitylsilane were recorded. Peaks observed matched exactly to literature values in all NMR spectra.

Scheme 1: Synthesis of trimesitylsilane.

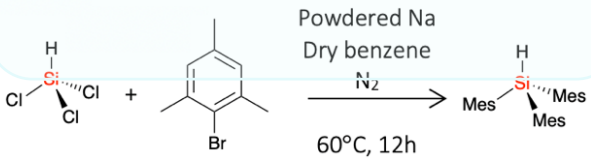

Lappert *et al.*[4]

Figure 2 - White crystals of trimesitylsilane, first batch (left) and second batch (right).

A sample of trimesitylsilane $SiH(Mes)_3$ was submitted for variable temperature single crystal X-ray diffraction (XRD). The crystal structure and unit cell are shown in Figure 3 and Figure 4, respectively. In the crystal structure the two mesityl (Mes) groups lay flat along the plane of the silicon centre and the third mesityl group sticks out of the plane to help minimise steric hindrance. The silicon atoms also keep the centre of the unit cell unoccupied to lower the lattice energy of the crystal. I expect that this space in the unit cell will be filled with anions when this compound Is used as a starting material to synthesise new ionic liquids. A second sample will be submitted for powder X-ray diffraction. Powder XRD will help to determine whether the crystal structure is representative of the bulk of the sample.

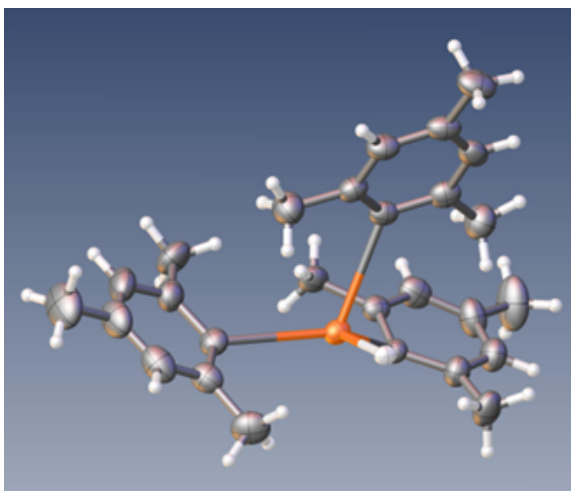

Figure 3 - Crystal structure of trimesitylsilane $SiH(Mes)_3$.

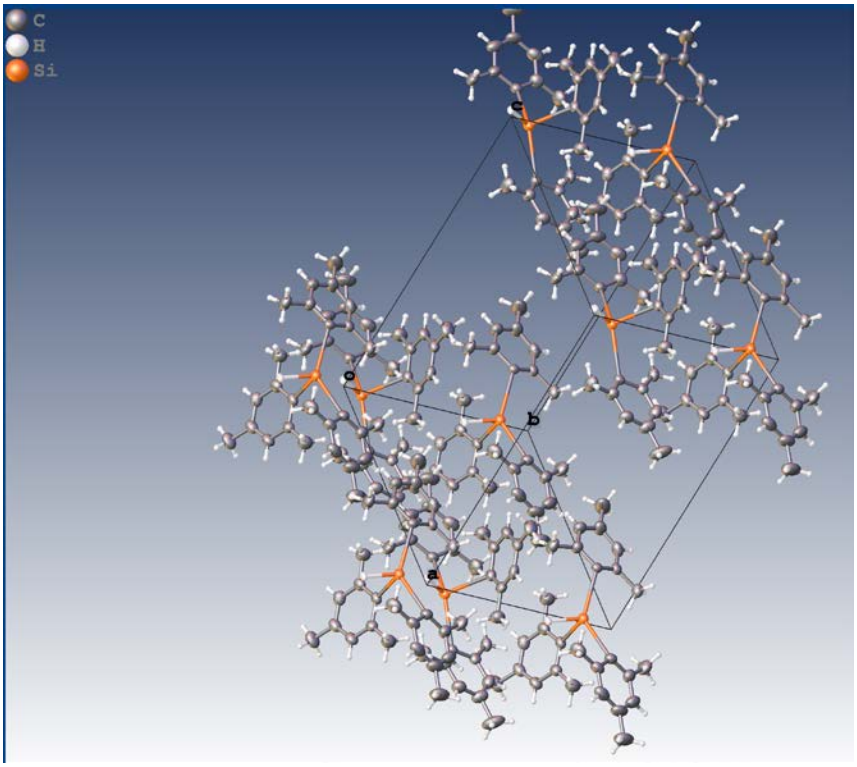

Figure 4 - Unit cell of trimesitylsilane $SiH(Mes)_3$.

Synthesis of $[Si(Mes)_3][NTf_2]$:

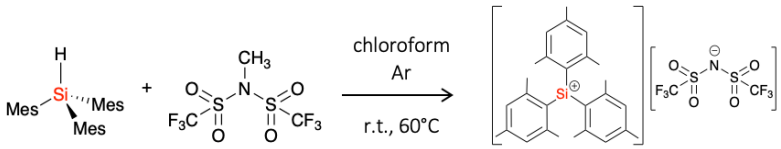

Scheme 2 - Synthesis of trimesitylsilylium bis[(trifluoromethyl)sulfonyl]imide $[(Mes)_3Si][NTf_2]$.

The synthetic route, illustrated in Scheme 2, will be repeated using air-sensitive techniques to generate trimesitylsilylium bis[(trifluoromethyl)sulfonyl]imide (bistriflimide), $[(Mes)_3Si][NTf_2]$. The trimesitylsilane starting material was synthesised following the method described previously by Lappert *et al.*[4] Trimesitylsilane will be reacted with n-methyl bis[(trifluoromethyl)sulfonyl]imide ($Me[NTf_2]$) and refluxed under argon in chloroform at 60 °C. The progress of the reaction will be monitored using ^{1}H, ^{13}C and ^{29}Si NMR. The product will be purified once there is no trimesitylsilane present in the NMRs. This new synthetic route will also be adapted in an attempt to generate a similar compound, trimesitylsilylium trifluoromethanesulfonate ($[Si(Mes)_3][OTf]$).

Conclusions and future work

Synthesis of $[Si(Mes)_3][OTf]$:

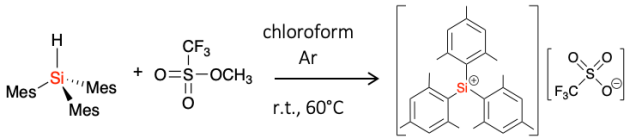

Scheme 3 - Synthesis of trimesitylsilylium trifluoromethanesulfonate $[Si(Mes)_3][OTf]$.

The synthetic route, illustrated in Scheme 3, was proposed to generate trimesitylsilylium trifluoromethanesulfonate (triflate), $[Si(Mes)_3][OTf]$. The trimesitylsilane starting material will be reacted with methyl trifluoromethanesulfonate (Me[OTf]) and refluxed under argon in chloroform at 60 °C. The progress of the reaction will be monitored using ^{1}H, ^{13}C and ^{29}Si NMR. The product will be purified and recrystallised once there is no trimesitylsilane present in the NMRs.

Characteristic Studies:

The crystals of $[(Mes)_3Si][NTf_2]$ obtained from the reaction in Scheme 2 were previously characterised using multiple analytical techniques, including thermogravimetric analysis (TGA), differential scanning calorimetry (DSC) and single crystal X-ray diffraction (XRD). These characterisation studies will be repeated with samples being prepared in a glovebox and air-sensitive techniques used when possible, for example, closed pan TGA. Further characterisation studies will be conducted including powder X-ray diffraction (PXRD) and mass spectrometry (MS). The kinematic viscosity and density of the compound will also be determined using a Stabinger viscometer (SVM).

If the synthetic route, illustrated in Scheme 3, successfully generates $[Si(Mes)_3][OTf]$, a complete characterisation study of the compound will be conducted. These analytical techniques will include closed pan TGA, DSC, single crystal XRD, PXRD, MS and SVM. Once again, these characterisation studies will be conducted with samples being prepared in a glovebox and air-sensitive techniques utilised if possible.

References

1. K. C. Kim, C. A. Reed, D. W. Elliott, L. J. Mueller, F. Tham, L. Lin and J. B. Lambert, *Science.*, 2002, **297**, 825–827.
2. J. B. Lambert and L. Lin, J. Org. Chem., 2001, **66**, 8537–8539.
3. A. Schäfer, M. Reißmann, S. Jung, A. Schäfer, W. Saak, E. Brendler and T. Müller, Organometallics, 2013, **32**, 4713-4722.
4. M. J. S. Gynane, M. F. Lappert, P. I. Riley, P. Rivière and M. Rivière-Baudet, J. Organomet. Chem., 1980, **202**, 5-12.

QUILL Quarterly Report

November 2022 – January 2023

Name:	Beth Murray		
Supervisor(s):	Prof Małgorzata Swadźba-Kwaśny and Prof John Holbrey		
Position:	PhD		
Start date:	October 2022	**Anticipated end date:**	October 2025
Funding body:	Department of Economy		

Liquid Coordination Complexes for the Synthesis of Semiconductor Nanoparticles

Background

My current work is based on the continuation of my MChem project, that focuses on the recovery of gallium metal from the zinc manufacturing industry, specifically zinc leachate solution, using hydrophobic deep eutectic solvents (DESs).

Global demand for gallium has rapidly increased over the past two decades, due to its applications in electronic devices. Challenges in its supply are exasperated by the lack of gallium ore, with this metal being recovered as a secondary element from mine tailings of other metal industries, chiefly aluminium, although recovery from zinc mine tailings is also potentially possible.[1] Finally, gallium supply is endangered by geopolitical consideration, with the majority being supplied by China (80%).[2]

As mentioned, this work focuses on the separation of gallium from zinc leachate solution, due to in Northern Ireland, this route of recovery being of great interest, on account of Europe's largest zinc mine being located in County Meath, Ireland.[3]

Hydrophobic DESs are based on the knowledge of hydrophobic ionic liquids and share similar characteristics such as long alkyl chains to promote hydrophobicity, however, are deemed less challenging and cheaper to prepare.[4] Previous literature on hydrophobic deep eutectic solvents (DESs) present hydrogen bond acceptor (HBA) molecules in combination with hydrogen bond donor (HBD) molecules, such as a carboxylic acid. A HBA molecule of great interest is trioctylphosphine oxide (TOPO), due to its application as a metal extractant in industry,[5] as well as its long alkyl chains which promote hydrophobicity. Although TOPO is used in aqueous organic liquid-liquid extractions, a major limitation to the process is its low solubility in hydrocarbon solvents, such as kerosene,[6] which are the chosen solvents for industrial extraction processes. By incorporating TOPO into a DES, it allows for large amounts of the phosphine molecule to be concentrated in the liquid form.

Objective of this work

The aim of this work is to explore hydrophobic DESs as a possible route for the extraction and recovery of gallium from the zinc manufacturing industry. Our strategy relies on the use of hydrophobic DESs as cost-effective, bifunctional solvents for the extraction of gallium. The overall aim is to find a system that results in the optimum amount of gallium being recovered,

along with high gallium selectivity over competitive metals in the simulated zinc leachate. Once I have completed all laboratory work on gallium separations and whilst continuing to write a paper for publication, I plan to also start on the nanoparticle section of my work. For this part of my project the aim is to develop new liquid coordination complexes (LCCs) and investigate them as precursors for the synthesis of semiconductor nanoparticles. This will include the synthesis and spectroscopic characterisation of firstly Ga/In selenide nanoparticles, before looking at ternary LCCs as precursors for nanoparticle synthesis.

Progress to date

We have developed a family of DESs based on trioctylphosphine oxide (TOPO), in combination with a selection of benign and inexpensive small organic molecules, that can act as cooperative complexing agents and/or reducing agents. These mixtures are then tested for the extraction and recovery of gallium from a simulated zinc leachate solution, where small (36 ppm) quantities of gallium are present, accompanied by very large quantities of other metals.

Initially, energy dispersive x-ray fluorescence (ED-XRF) had been used to determine the metal concentration of the aqueous phase pre-extraction, post-extraction and post-metal stripping. This was done by preparing several multi-metal stock solutions in 6M HCl, with decreasing metal concentration, allowing a calibration curve for each metal present in the zinc leachate to be created by empirical analysis (EMP) on ED-XRF. After several months of furthering my knowledge on this method, the decision has now been made to use XRF as a screening technique for results, before using inductively coupled plasma optical emission spectroscopy (ICP-OES) for accurately determining the metal concentration in the aqueous phase. Due to aluminium being one of the metals usually co-extracted and stripped alongside gallium, it is important to be able to accurately determine the amount of aluminium recovered from the zinc leachate solution. This is crucial in being able to calculate separation factors and demonstrate the selectivity of the system. One of the drawbacks of ED-XRF analysis is the difficulty in measuring lighter elements, such as aluminium, as its fluorescence struggles to reach the detector, making it difficult for the instrument to accurately determine how much of the element is present.

A TOPO:malonic acid system ($\chi_{TOPO} = 0.60$) has been shown to successfully extract, and recover gallium from a zinc leachate solution (16.5 ppm). A drawback of this system, however, is low selectivity towards gallium with aluminium, iron and copper also being recovered. Further systems have been tested with the aim of improving selectivity, including a TOPO:erythorbic acid ($\chi_{TOPO} = 0.68$) eutectic. This system resulted in higher gallium selectivity, due to preventing the recovery of copper in the stripped aqueous phase; speculated to be a result of Cu(II) being reduced to Cu(I),[7] therefore, chemically dissimilar from Ga(III).[8]

The latest development in this work has been the addition of a small concentration of ascorbic acid (0.15 mol dm^{-3}) to the TOPO:malonic acid system ($\chi_{TOPO} = 0.60$). Ascorbic acid (vitamin C) is a known natural reducing agent,[9] that has the potential to reduce Fe^{3+} to Fe^{2+} and/or Cu^{2+} to Cu^{+}.[10] By reducing iron and copper, it is speculated both metals are converted into less easily recovered versions and thus susceptible to co-stripping. As gallium is most likely present in the form of the tetrahedral $[GaCl_4]^-$ species in 6 M HCl solution,[11] by reducing iron to its +2 oxidation state, and copper to its +1 state, this will result in their tetrahedral ionic

radii being more dissimilar to Ga^{3+} tetrahedral ionic radii. The ionic radii of these ions are shown in Table 1. The amount of gallium also recovered is a lot greater when ascorbic acid is added to the system in comparison to when ascorbic acid is absent (27.5 ppm and 8.4 ppm respectively).

Table 1 - Tetrahedral ionic radii of gallium, iron and copper ions.[8, 12]

Metal ion	Tetrahedral ionic radii / Å
Ga^{3+}	0.47
Fe^{3+}	0.49
Fe^{2+}	0.63
Cu^{2+}	0.57
Cu^{+}	0.60

Conclusions and future work

From this work good progress has been made regarding the recovery of gallium from a simulated zinc leachate solution, however, there is still a comprehensive amount of future work that could be carried out.

Firstly, the identification of eutectic mixtures was completed in the screening study of various HBDs in combination with TOPO. This allowed for the eutectic mixtures to be scaled up and tested as extractants for gallium from a simulated zinc leachate solution. Although in the extraction study, the eutectic systems in this work showed high metal coextraction, therefore, demonstrating low selectivity towards gallium, the benefits of these systems are later highlighted in the metal stripping studies. Both TOPO:malonic acid (χ_{TOPO} = 0.60), and TOPO:erythorbic acid (χ_{TOPO} = 0.68) systems have been shown to successfully recover gallium from a simulated zinc leachate solution. It has also been shown that the addition of a low concentration of ascorbic acid (0.15 mol dm^{-3}) to the TOPO:malonic acid system (χ_{TOPO} = 0.60) improves the selectivity of the system, by reducing the amount of iron and copper also recovered alongside gallium, whilst remaining to give high gallium selectivity over aluminium, indium and zinc.

Future work plans include finishing off the gallium separation work, with the aim of publication. This includes possibly completing mixer-settler extraction tests, as well as altering the concentration of ascorbic acid to the TOPO:malonic acid system, to see if further selectivity improvements can be made. After completing all lab work required on the Ga separation studies and whilst writing, I will begin work on the LCC work. This will first start off with the synthesis of Ga/In selenide nanoparticles to allow for spectroscopic studies.

1. F. Lu, T. Xiao, J. Lin, Z. Ning, Q. Long, L. Xiao, F. Huang, W. Wang, Q. Xiao, X. Lan and H. Chen, *Hydrometallurgy*, 2017, **174**, 105-115.
2. E. Commission, *Report on Critical Raw Materials for the EU. Report of the Ad hoc Working Group on defining critical raw materials.*, EU, Brussels, 2014.
3. E. L. Byrne, R. O'Donnell, M. Gilmore, N. Artioli, J. D. Holbrey and M. Swadźba-Kwaśny, *Phys. Chem. Chem. Phys.*, 2020, **22**, 24744-24763.
4. M. Gilmore, L. M. Moura, A. H. Turner, M. Swadźba-Kwaśny, S. K. Callear, J. A. McCune, O. A. Scherman and J. D. Holbrey, *J. Chem. Phys.*, 2018, **148**, 193823.
5. T. Sato, T. Nakamura and H. Oishi, *Solvent Extr. Ion Exch.*, 1984, **2**, 45-60.

6. E. K. Watson, W. A. Rickelton, A. J. Robertson and T. J. Brown, *Solvent Extr. Ion Exch.*, 1988, **6**, 207-220.
7. O. Naoyasu, N. Yuzo, I. Kazuhiko and K. Sigeo, *Bull. Chem. Soc. Jpn.*, 1980, **53**, 2847-2850.
8. R. D. Shannon, *Acta Cryst.*, 1976, **A32**, 751-767.
9. D. Njus, P. M. Kelley, Y.-J. Tu and H. B. Schlegel, *Free Radical Biol. Med.*, 2020, **159**, 37-43.
10. A. Elmagirbi, H. Sulistyarti and A. Atikah, *J. Pure App. Chem. Res.*, 2012, **1**, 7.
11. L. A. Woodward and A. A. Nord, *J. Chem. Soc.*, 1956, **0**, 3721-3722.
12. W. Xie, F. M. Allioux, J. Z. Ou, E. Miyako, S. Y. Tang and K. Kalantar-Zadeh, *Trends Biotechnol*, 2021, **39**, 624-640.

QUILL Quarterly Report

November 2022 – January 2023

Name:	Hugh O'Connor		
Supervisor(s):	Prof Peter Nockemann, Dr Steve Glover and Dr Josh Bailey		
Position:	PhD Student		
Start date:	October 2019	**Anticipated end date:**	March 2023
Funding body:	EPSRC		

Redox Flow Battery Materials for Energy Storage

Background

As fossil fuel supplies dwindle and the climate change problem escalates, the need to harness renewable energy resources increases. However, these energy sources are intermittent and unpredictable, making them difficult to be used in a safe and stable power grid. For this reason, it is important that new energy storage technologies are developed which can shift energy from off-peak demand times to peak demand times. One of the most promising emerging technologies is the redox flow battery (RFB).

In RFBs, redox couples are dissolved in electrolyte solutions and stored in separate reservoir tanks. During charge and discharge these electrolytes are pumped from reservoir tanks into half cells where they react in an electrode, either consuming or generating electrons.

This working principle gives rise to a number of key advantages over other conventional battery technologies. In flow batteries, power and energy is decoupled; power is controlled by the stack effectiveness whilst energy is stored in the electrolyte reservoir tanks. This makes RFBs highly customisable, allowing them to be tailored to meet the demands of various power grids. They also have a long working life; with the electrolytes stored in separate tanks, the electrodes don't undergo complex redox reactions and experience less structural changes and strain than those found in conventional batteries. One drawback of RFBs however is their low energy density and high costs when compared to other energy storage technologies.

Improving the energy density, energy storage efficiency and sustainability could make RFBs an even more promising candidate for large scale energy storage applications. Innovative and more efficient manufacturing techniques could also potentially provide a solution in reducing inevitable costs that will occur when implementing a new energy storage technology.

One method of improving the performance of RFBs is designing better performing flow fields, manifolds and topologies to improve mass transport of the reactant, reducing concentration overpotentials resulting in a better performing cell with higher voltage efficiencies.

Objective of this work

To investigate the effect of modified cell topology on the performance of redox flow batteries, identifying key performance influencers and improving economic viability.

Progress to date

During the early stages of my research, 3D-printing was identified as a powerful tool in the development of laboratory scale redox flow battery cells that can be used to develop new electrolyte technologies or materials. This platform has been utilised to test a wide range of flow battery materials (including various electrodes, membranes and gaskets) as well as the evaluation of new electrolyte technologies. It has also been used to generate miniaturised cells to carry out in-situ micro X-ray CT imaging at the Diamond light source synchrotron. An in-depth study into flow battery test procedure and reproducibility of results has been carried out using the 3D-printing platform, revealing a number of important parameters to consider when testing flow batteries. The learnings from this study are now being applied to the evaluation of a number of previously untested, modified cell topologies. These new topologies aim to increase the voltage efficiency and power density of flow-through cells by improving the distribution of electrolyte through the electrode cavity compared to conventional flow through cells. Simulations are also being carried out using a coupled electrochemical/ computational fluid dynamics model to predict the performance of these cells and other topologies at a range of operating conditions.

Conclusions and future work

The effect of cell design on the performance of flow through redox flow batteries has been investigated using a combined approach of 3D-printing, laboratory testing and electrochemical/ computational fluid dynamics simulation. 3D-printing has also been used to develop new test procedures in order to generate repeatable data. Work is ongoing to further develop the model used for simulations as well as the testing of a range of different cell topologies.

Publications

O'Connor et al., An open-source platform for 3D-printed redox flow battery test cells, RSC Sustainable Energy & Fuels, 10.1039/d1se01851e.

QUILL Quarterly Report

November 2022 – January 2023

Name:	Liam O'Connor		
Supervisor(s):	Dr O Istrate and Prof B Chen		
Position:	PhD student		
Start date:	01st Oct 2020	**Anticipated end date:**	30th Sept 2023
Funding body:	Department for the Economy		

3D-Printed Polymer Graphene Nanocomposites for Biosensor Applications

Background

A polymer strain sensor works on the principle that the electrical conductivity is proportional to the mechanical strain applied. Thus far, literature has focused on the prosthetic using feedback from pressure sensors in the fingertip to give feedback to the user. One of the limitations of using this pressure sensor is that it can only distinguish objects within the surface area of the sensors, which is 15 mm2. A solution to the limitation of pressure sensors is to develop a strain-dependent electrically conducting material and coat the outer material of the prosthetic. An important feature of the material used to manufacture a prosthetic arm is that it needs to be 3D printable. 3D printing of the prosthetic arm is required because there is no standard size for a person's arm. The materials being investigated are thermoplastic polyurethane (TPU) because of its strong hysteresis response to mechanical strain, nylon-11 (PA11) because of its piezoelectric properties, and graphene nanoplatelets (GNP) because it is shown to increase the electrical conductivity of other piezoelectric polymers, such as polyvinylidene fluoride (PVDF) at 25 wt.% (weight per cent).

Objective of this work

The work aims to develop a strain-dependent electrically conducting material that can be used as a strain sensor and be FDM 3D printed. This will be done by determining the optimal graphene for the manufacturing of TPU/GNP filaments, determining the optimal graphene loading for the manufacturing of PA11/GNP filaments, determining the optimal graphene loading for the manufacturing of TPU/PA11/GNP filaments, and determining the optimal manufacturing layering for TPU/PA11/GNP filaments.

Progress to date

The TPU/PA11/GNP nanocomposite have been mechanically and electro mechanically analysed. SEM images of the TPU/GNP and PA11/GNP have been collected. The 3D printing conditions of the TPU/GNP and PA11/GNP composite have been calibrated.

Conclusions and future work

The TPU/PA11/GNP blend is ductile, like the TPU/GNP composite. It has an electrical percolation threshold like the PA11/GNP composite. PA11/GNP composite at 10wt. % showed an electric response to mechanical strain applied whereas the blended composite did not show any electric response to mechanical strain. The next stage of the project is to 3D print

the blended composite and collect SEM images of blended composite and evaluate the piezoelectric properties of the PA11/GNP and TPU/PA11/GNP

QUILL Quarterly Report

November 2022 – January 2023

Name:	Scott Place		
Supervisor(s):	Dr Paul Kavanagh (Primary) and Dr Mark Muldoon (Secondary)		
Position:	PhD Student (4th Year)		
Start date:	Oct 2019	**Anticipated end date:**	Sep 2023
Funding body:	EPSRC		

Molecular Electrocatalysts for Energy and Electrosynthetic Applications

Background

This project focuses on the nitroxide radical molecule, TEMPO, and its derivates, their electrokinetic properties, and their applications in energy storage, energy generation, and electrosynthetic applications. TEMPO-like molecules can be electrochemically oxidised at an electrode surface to an active oxoammonium form, which can then react with substrates in a chemical redox reaction, which regenerates them to their nitroxide (or hydroxide, when protons are present) form. These reactions follow the well-established EC' (electrochemical-chemical) two-step reaction profile, studied extensively by Savéant and co-workers and Dempsey and co-workers, among others.

Electrolysis for organic synthesis is gaining popularity in the literature as a low-waste and simple procedure for converting a number of substrates to their corresponding products. TEMPO and its derivatives are an example of chemicals that can be used as electrocatalysts for oxidation reactions, where direct electrochemical oxidation of the substrate may be too energy intensive.

Objective of this work

The aim of this work is to use TEMPO and its derivatives as a case-study for the application of electroanalytical techniques for use in synthetic organic chemistry. Since electrochemistry and organic chemistry are typically divergent paths from an early stage in most chemist's careers, there is a language-barrier of sorts between the two fields. Here we aim to show how electroanalytical techniques can be used to benchmark electrocatalyst performance, highlighting key considerations to take during the analysis.

Progress to date

In my previous report, I discussed the challenges faced in experimental reproducibility and the solutions put in place to minimise them. Additionally, it was highlighted that the status quo of catalytic Tafel plots for showcasing molecular electrocatalysts may be misleading.

Since then, during our longer-term analysis using chronoamperometry and chronopotentiometry, we have discovered that TEMPO/NMI alcohol electro-oxidation in MeCN is impractical, where all catalysts fail to drive the reaction beyond 30-40% completion before complete loss of current is observed. Though frustrating, this is an important finding.

It was entirely possible to produce a catalytic Tafel plot for these catalysts in this system, supposedly highlighting some as “good” or “bad” catalysts, with no obvious indication that all catalysts in the line-up would be unsuitable for this reaction. Our work here pointedly highlights the risks of relying exclusively on Tafel plots and similar work when choosing catalysts, and the necessity of longer-term analytical techniques such as chronoamperometry.

It is still our intent to demonstrate an appropriate regime for benchmarking catalysts for a fully-functional system, and so we have moved our focus to TEMPO-derivative alcohol oxidation reactions in pH 10 carbonate buffer systems, which is well-established as an appropriate system for high conversions. Work is currently underway to reproduce a high conversion electrosynthesis of benzaldehyde from benzyl alcohol in aqueous media.

Conclusions and future work

If the current work on aqueous electrosynthesis is successful, we will move onto applying this system to the other derivatives of TEMPO which have been the focus of our work in organic media. We will:

- Thoroughly establish pure kinetic conditions for these catalysts in this aqueous solvent system.
- Estimate a series of rate constants for these catalysts using the Savéant framework.
- Produce an appropriate Tafel plot as per the status quo of benchmarking catalysts.
- Design a series of long-term electrolysis experiments, backed up by GC analysis, to demonstrate differences in catalyst stability and real-world performance, highlighting and correlations to and limitations of the Tafel plot data.

QUILL Quarterly Report

November 2022 – January 2023

Name:	Junzhe Quan		
Supervisor(s):	Prof John Holbrey and Dr Leila Moura		
Position:	PhD Student		
Start date:	01/10/2019	Anticipated end date:	01/10/2023
Funding body:	Self funding		

Use Ionic Liquids that Exhibit LCST (Lower Critical Solution Temperature) Behaviour as Draw Fluids for Water Treatment, Desalination and Separation

Background

New Ionic liquid materials have been recently developed that exhibit lower critical solubility temperature (LCST) behaviour with water. That is, they are miscible at a low temperature and split into two aqueous phases on heating beyond a critical temperature. Such materials have the potential to be used as draw fluids for forward osmosis (FO) water desalination using low grade energy to address the global challenge to provide clean, accessible drinking water to all the world's populations. In this research , new ionic liquids will be investigated as advanced fluids for forward osmosis water treatment. This offers opportunities to advance less energy intensive alternative to conventional reverse osmosis as a solution to the global challenge of providing potable water in regions of low availability.

Objective of this work

My research program in the use of ionic liquids as potential draw fluids for FO water treatment includes:

1. Preparation of appropriate model tetrabutylphosphonium/ammonium ionic liquids
2. Characterisation of aqueous/ionic liquid phase behaviour as a function of aqueous component salinity, pH, temperature and to draw structure-performance relationships with the ionic liquid cation/anion components
3. Develop a FO membrane cell system to test and evaluate draw fluid characteristics and parameters of selected systems
4. Optimize ionic liquid to use as draw fluid, developing a proof-of-concept ionic liquid-based FO desalination demonstrator for benchmarking
5. Examine the applicability of these draw fluids to water-processing of a range of feeds and product streams (desalination, waste concentration, biomass dewatering)
6. Measure the energy consumption and compare with typical method of water treatment

Progress to date

A large quantity of thermos-sensitive ionic liquid $[P_{4444}][TsO]$ and $[P_{4444}][Ph\text{-}tet]$ has been prepared and fully characterized by NMR, FT-IR and TGA. $[P_{4444}][TsO]$ and $[P_{4444}][Ph\text{-}tet]$ have been tested by FO performance test system twice and a range of data were outputted.

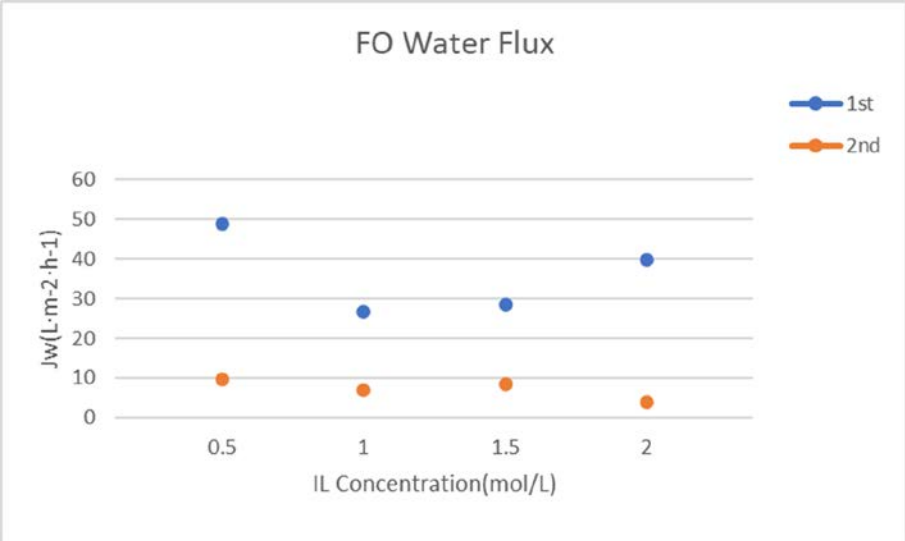

Figure 1 - Water flux data of [P_{4444}][Ph-tet] system

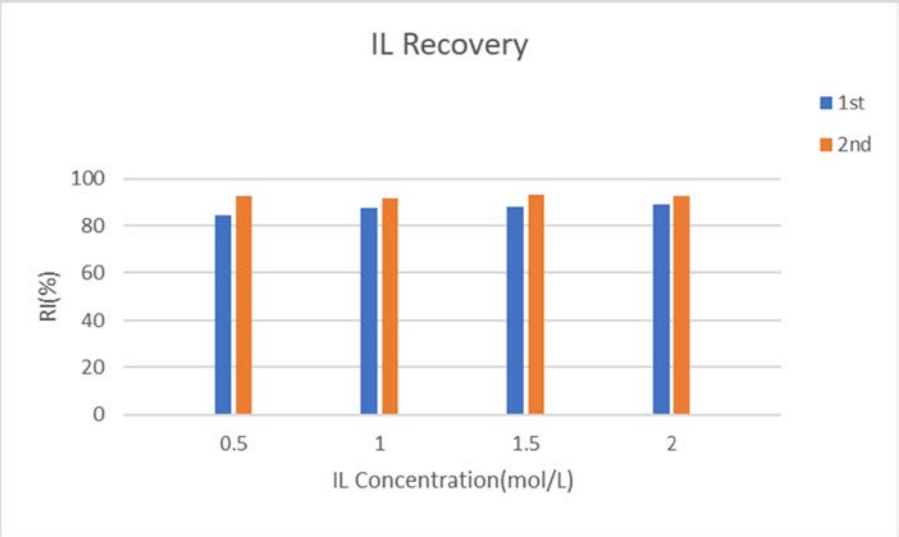

Figure 2 - Ionic liquid recovery of [P_{4444}][Ph-tet]

Conclusions and future work

After the first experiment, we found that the system has a major mechanical error because the peristaltic pump can not pump all liquid in system out which resulting in the lower ionic liquid recovery and incorrect huge water flux data. In second experiment, an air blower was added to system in order to blow all the residual liquid in pump. The ionic liquid recovery increased obviously and the water flux data make sense.

About the future work, we plan to finish testing two materials([P_{4444}][TsO] and [P_{4444}][Ph-tet]) in this system and compare their FO performance. We also need to output the reverse solute flux data and calculate each ionic liquid/water system's FO performance. Then, we will focus on test more LCST type IL materials to select and optimize the best one for different industry application. After testing these thermo-sensitive ILs, we can also test some other kinds of draw solutes just like switchable CO_2-stimuli materials. Then compare them to explore the difference between them to show IL draw solute's advantages.

QUILL Quarterly Report

Nov 2022 – Jan 2023

Name:	Richard Woodfield		
Supervisor(s):	Dr Stephen Glover and Prof Peter Nockemann		
Position:	PhD Student		
Start date:	03/06/2019	**Anticipated end date:**	03/05/2023
Funding body:	EPSRC		

Modelling Vanadium Redox Flow-Batteries in Transport Applications

Background

Flow batteries have received significant attention in the past years for use in grid storage applications. The decoupling of the relationship between power and energy density offers a very unique way to store energy to suit the user's particular needs. The extremely long cycle life of a flow-battery is another attractive asset, as the electrodes do not undergo cyclic stressing in the same way Li-ion and other chemistries do. Flow-batteries have received very limited attention regarding their use in transport applications. There is untapped potential in the fact that the discharged electrolyte of a flow-battery could be rapidly swapped at a traditional gas-station, where the infrastructure is already half in-place with storage tanks under the stations. With the electrolyte being entirely re-usable, the station would use an on-site flow-battery to recharge their reservoir and provide passing vehicles with opportunity to swap their electrolyte with readily charged fluid.

Objective of this work

The overall goal of the project is to identify viable electric or hybrid modes of transport that would benefit from the use of a flow-battery, given the refillable nature of the flow-battery electrolyte reservoirs. Even the applications rendered not viable will have outcomes, as the amount by which the energy density of the electrolyte would need to improve by is also providing electrolyte chemists with targets to aim for. The investigations will be carried out using software to model battery and vehicle behaviour, primarily Simulink.

Progress to date

To date work has been published on the use of vanadium redox flow batteries in ferry applications in the journal of energy storage:
https://www.sciencedirect.com/science/article/pii/S2352152X22013044

Conclusions and future work

Modelling work has begun investigating the use of vanadium redox flow batteries in hybrid bus applications, where initial models show promise. Over the lifetime of the bus, hybridizing vanadium redox flow-batteries with fuel cells shows a cost reduction versus pure fuel cell buses. This study will now continue to explore other bus scenarios in order to make a fair comparison, and then will be published in the coming months.

QUILL Quarterly Report

November 2022 - January 2023

Name:	John Young		
Supervisor(s):	Dr Leila Moura, Prof John Holbrey and Prof Sophie Fourmentin		
Position:	PhD student		
Start date:	2020	Anticipated end date:	2024
Funding body:	EPSRC		

Gas Separation Technologies

Background

Biogas is a renewable and carbon neutral energy source obtained through anaerobic digestion (AD) of organic waste. Biomethane is obtained through the upgrading of biogas produced from anaerobic digesters. It consists of mainly methane and carbon dioxide with many trace compounds including hydrogen sulfide, ammonia, silioxanes, terpenes and water vapour. Biomethane must be of a purity equal to or better than that of natural gas if it to be utilised for grid injection therefore a methane purity of above 96% must be achievable from any prospective technology. Carbon dioxide should make up 2.5-4% of the remaining volume with contaminants such as sulfur and siloxanes being limited to 10 mg/m^3 and 0.1 mg/m^3 respectively. The primary focus of this research is on carbon dioxide/methane separation as these are the two major components of biogas.[1]

Currently biogas upgrading is multistep, with scrubbing used for carbon dioxide removal from the biogas stream to concentrate methane. This involves the use of liquid amines such as MEA (monoethanolamine) where carbon dioxide is captured through a chemisorption process. Regeneration of the amines requires high energy inputs in the form of steam at 100-150^oC to reform the initial liquid amine. Water scrubbing can also be used but this requires large amounts of water and leads to methane slip due to the lower selectivity of water compared with other technologies. Membranes offer another option for upgrading but these also suffer from a range of issues such a low throughput coupled with fouling and plasticisation. The degradation of membranes leads to issues both economically in the form of having to replace them but from an environmental standpoint it is unsustainable to continuously have to dispose of and manufacture replacement membranes. Cryogenic distillation offers a method of using nontoxic materials to produce high purity gas streams through the utilisation of low temperatures and high pressures which allows carbon dioxide to liquefy leaving a pure methane stream. However the energy cost associated with this method is massive which makes it less sustainable and exceedingly costly.[2]

It is for these reasons that we seek to create novel materials which will be more efficient, more sustainable and economically viable for biogas upgrading. Initial work will consist of the use of deep eutectic solvents in conjunction with other materials to increase their upgrading capabilities.

Work to date

Gas screening methodology

Measurements to quantify the gas capacity and selectivity of both liquids and solids can be painstakingly slow and have a high associated cost. I have been developing a headspace GC (HS-GC) methodology to quickly screen liquid and solid sorbent materials for their gas capacity and separation ability. The screening can be performed at a range of pressures and temperatures, with a variety of pure gases and mixtures of gases. To do this I tested multiple combinations of HS-GC vials, stoppers and caps, resulting in the combination described in Figure 1. The idea is to use the vials as mini equilibration vessels in which PVT based measurements can occur. These measurements are not expected to be as accurate as other methods, but we expect them to serve for screening purposes.

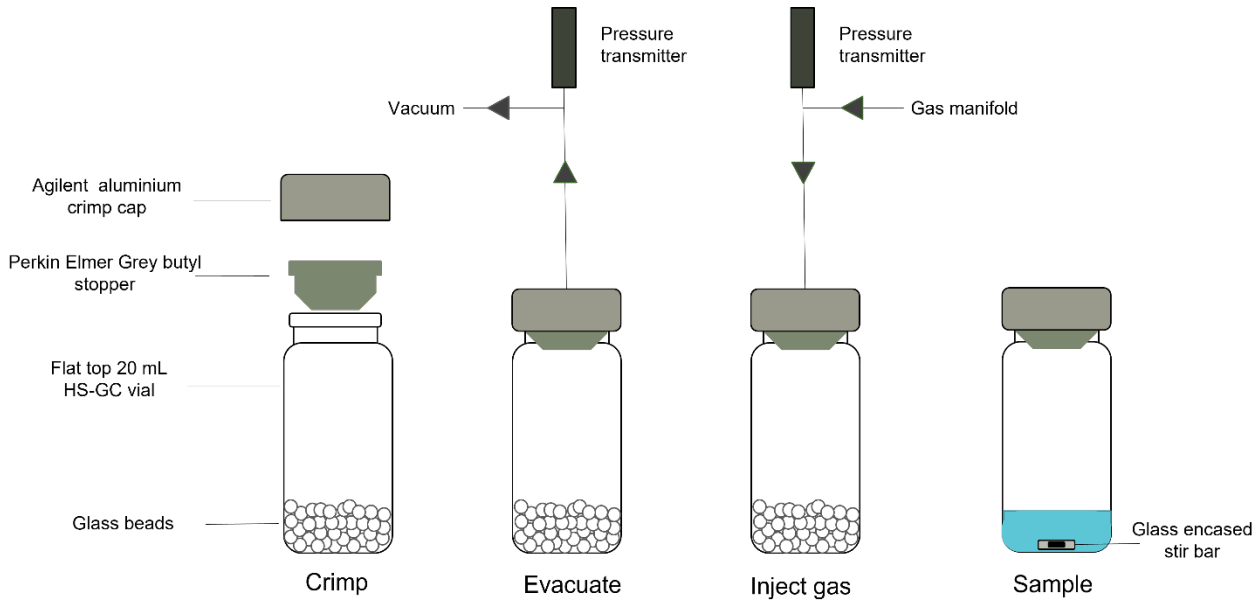

Figure 1 - Schematic of HS-GC vial preparation for calibration (glass beads) or for gas uptake measurements with sample (blue liquid)

By injecting a known "initial pressure" (quantity determined by PV calculations) of pure gas into an evacuated HS-GC vial we can compare the peak area associated with the injected gas from a calibration curve to the recorded peak area after equilibration with a known sorbent. The pressure difference in these two values equates to the gas uptake. An example can be seen below in Figure 2 where a variety of CO_2 uptake isotherms of initial pressure against peak area shows that decreased peak areas can be seen in materials with a higher associated gas capacity.

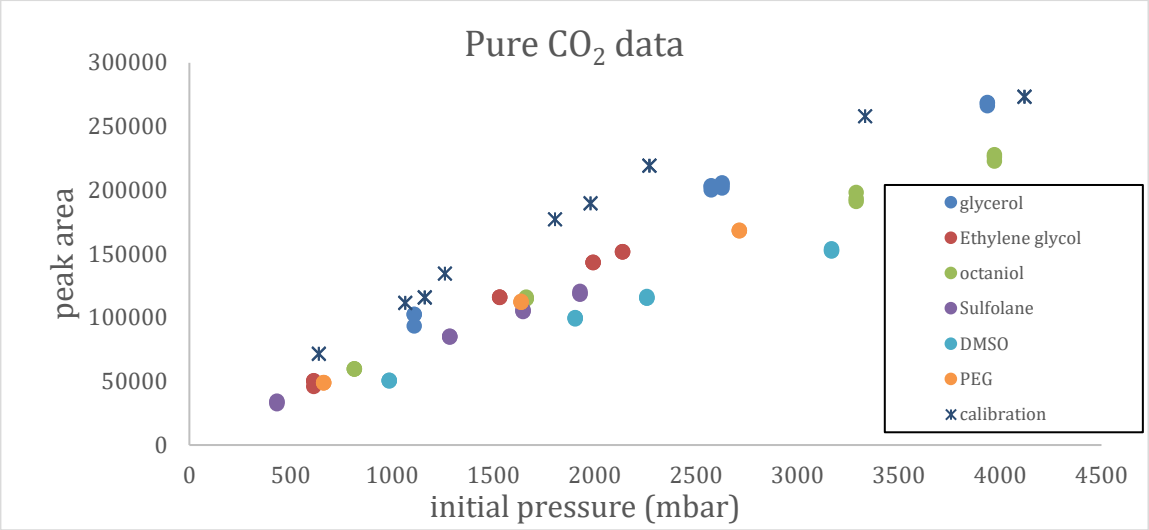

Figure 2 - Comparison of peak areas associated with different materials after equilibration with a known initial CO_2 pressure when compared to a calibration curve using glass beads

This data was then converted to mole fraction as a function of equilibrated pressure and compared to literature data for the same materials (Fig 3). It can be seen that the experimental gas capacities using this method are in good agreement with that of the literature data within the same pressure range.

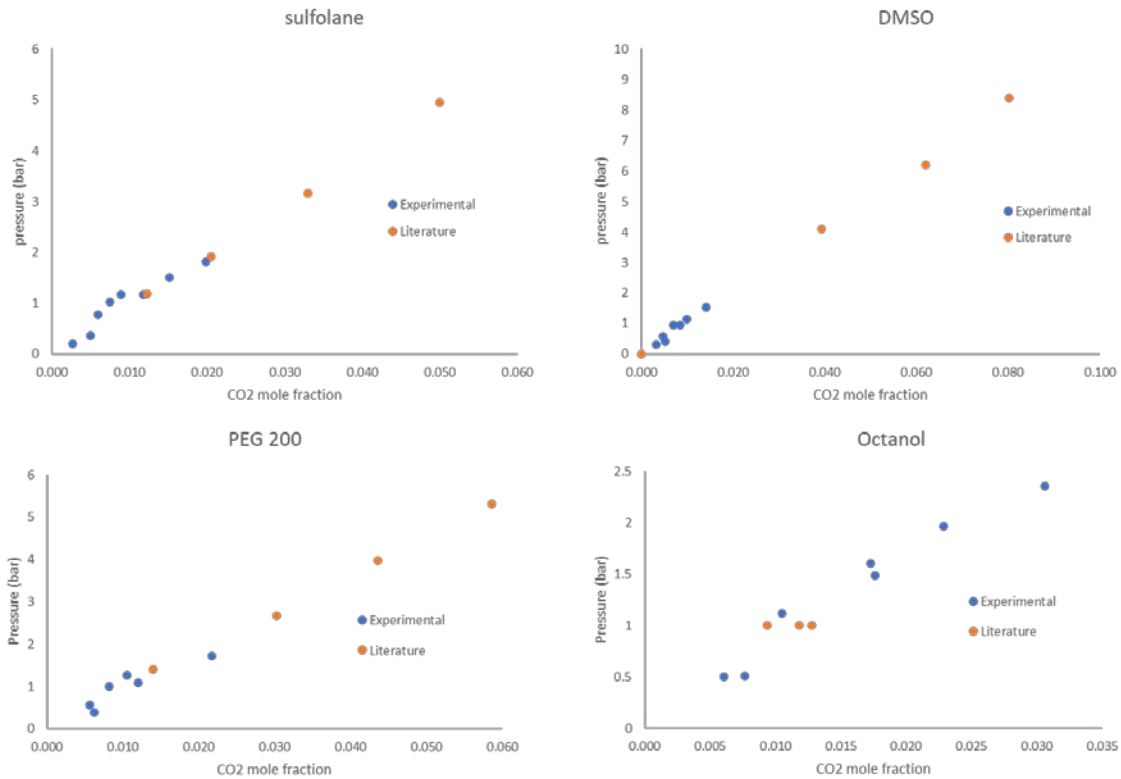

Figure 3 - Experimental uptake data of pressure against mole fraction of CO_2 obtained in this work (blue) when compared with uptake data from literature sources (orange) showing good agreement

Measurements like these have been carried out with CO_2, CH_4, C_2H_4 and C_2H_6 so far with both solid and liquid systems. These have also been found to yield results which compare well to that of literature. The error, accuracy and deviations from the literature data for these measurements is also being estimated.

Future work

More data must be collected and after which we will write a methodology based paper on this work to be published on. We would also like to be able to include hydrogen in this paper as a gas for which you can quantify. Due to the experimental difficulties associated in hydrogen detection and handling this has not been carried out yet but is underway.

References

1. F. M. Baena-Moreno, M. Rodríguez-Galán, F. Vega, L. F. Vilches and B. Navarrete, *Int. J. Green Energy*, 2019, **16**, 401–412.
2. M. R. Rodero, R. Ángeles, D. Marín, I. Díaz, A. Colzi, E. Posadas, R. Lebrero and R. Muñoz, in *Biogas*, Springer, 2018, pp. 239–276.
3. E. L. Byrne, R. O'Donnell, M. Gilmore, N. Artioli, J. D. Holbrey and M. Swadźba-Kwaśny, *Phys. Chem. Chem. Phys.*, 2020, **22**, 24744–24763.
4. R. Ullah, M. Atilhan, B. Anaya, M. Khraisheh, G. García, A. ElKhattat, M. Tariq and S. Aparicio, *Phys. Chem. Chem. Phys.*, 2015, **17**, 20941–20960.